

Review

Recent advances in fiber-shaped and planar-shaped textile solar cells



Mohammad Hatamvand ^{a,*}, Ehsan Kamrani ^{b,c}, Mónica Lira-Cantú ^d, Morten Madsen ^e, Bhushan R. Patil ^e, Paola Vivo ^f, Muhammad Shahid Mehmood ^a, Arshid Numan ^{a,g}, Irfan Ahmed ^{a,h}, Yiqiang Zhan ^{a,**}

^a Center of Micro-Nano System, School of Information Science and Technology, Fudan University, Shanghai, 200433, China

^b Center for Intelligent Antenna and Radio System (CIARS), Department of Electrical & Computer Engineering, University of Waterloo, Waterloo, ON, Canada

^c Wellman Center for Photomedicine, Harvard Medical School, Boston, MA, USA

^d Catalan Institute of Nanoscience and Nanotechnology (ICN2), CSIC and the Barcelona Institute of Science and Technology, Campus UAB, Bellaterra, E-08193, Barcelona, Spain

^e SDU NanoSYD, Mads Clausen Institute, University of Southern Denmark, Alsion 2, 6400, Sønderborg, Denmark

^f Faculty of Engineering and Natural Sciences, Tampere University, P.O. Box 541, FI-33014, Tampere, Finland

^g Graphene & Advance 2D Materials Research Group, Research Centre for Nanomaterials and Energy Technology, School of Science and Technology, Sunway University, 47500, Selangor, Malaysia

^h Department of Physics, Government Postgraduate College, Mansehra, 21300, (Higher Education Department-HED) Khyber Pakhtunkhwa, Pakistan

ARTICLE INFO

Keywords:

Fiber -shaped solar cells
Textile solar cells
Power harvesting
Smart textiles
Electronic textiles
Wearable electronic devices

ABSTRACT

During the last few years, textile solar cells with planar and fiber-shaped configurations have attracted enormous research interest. These flexible-type solar cells have a huge potential applicability in self-powered and battery-less electronics, which will impact many sectors, and particularly the Internet of Things. Textile solar cells are lightweight, super-flexible, formable, and foldable. Thus, they could be ideal power-harvester alternatives to common flexible solar cells required in smart textiles, electronic textiles, and wearable electronic devices. This review presents a brief overview on fiber-shaped and planar-shaped solar cells, and it introduces the most recent research reports on the different types of textile solar cells, including details on their fabrication techniques. It also addresses the current challenges and limitations of their technology development, and the encountered issues for their future application and integration in novel devices.

1. Introduction

Relying on fossil fuels for addressing the global energy demand is a key current concern for the society, as they lead to environmental pollution upon the release of carbon dioxide and other greenhouse gases. This results in global warming and climate changes, which are significant challenges in a world with a continuously growing population. Thus, the utilization of clean and renewable energy resources is an urgent and high-demand necessity. Solar energy is a promising alternative to fossil fuels as it is renewable, clean, eco-friendly, sustainable, abundant, and readily available. Hence, in the last decades, many research efforts have been devoted to improving the performance and the stability of emerging photovoltaic (PV) technologies, such as dye-sensitized [1–10], organic [11–24], and perovskite PVs [25–44]. While the conventional silicon solar cells are heavy, fragile, and rigid,

the above-mentioned latest PV technologies offer unique advantages over the silicon counterparts, namely the solution processability, the flexibility and their being lightweight. These features enable their integration in portable electronic applications. Recently, scientists have carried out significant research and development efforts to bridge the performance and stability gap of flexible solar cells [45–63]. Their photoactive materials should be able to generate high Power Conversion Efficiencies (PCE) while having at the same time excellent tolerance towards mechanical bending and stretching stress [64]. However, despite the progress of the latest years, flexible solar cells can still only endure a limited bending radius. This ultimately reduces their applicability in super flexible products, such as cases where formability, pliability, foldability, and wearability are requested, e.g. in Wearable Electronic Devices (WEDs). WEDs are typically battery-powered and mainly constructed on textile-based materials such as fibers and fabrics.

* Corresponding author.

** Corresponding author.

E-mail addresses: m_hatamvand@fudan.edu.cn (M. Hatamvand), yqzhan@fudan.edu.cn (Y. Zhan).

Table 1
Structure and PV parameters of different types of fabricated FSCs.

Structure	Type	J _{SC} (mA cm ⁻²)	V _{OC} (V)	FF	PCE (%)	Ref.
Ti wire/TiO ₂ NPL/N719/I ⁻ I ₃ ⁻ /Pt wire	DSSC	10.60	0.68	0.83	6.00	[74]
Ti wire/TiO ₂ CL/TiO ₂ NPL/N719/I ⁻ I ₃ ⁻ /Pt wire	DSSC	12.58	0.68	0.71	6.12	[82]
Ti wire/graphene-TiO ₂ /N719/I ⁻ I ₃ ⁻ /Pt wire	DSSC	6.09	0.75	0.70	3.26	[81]
Ti wire/aligned TiO ₂ nanotube arrays/N719/I ⁻ I ₃ ⁻ /MWCNT array	DSSC	16	0.71	0.61	7.13	[88]
Ti wire/TiO ₂ NPs/organic dye/I ⁻ I ₃ ⁻ /Pt wire	DSSC	7.54	0.64	0.64	3.12	[85]
Ti wire/TiO ₂ nanotube/N719/I ⁻ I ₃ ⁻ /Pt-coated carbon fiber	DSSC	11.92	0.74	0.64	5.64	[79]
Ti wire/TiO ₂ nanotube arrays/N719/I ⁻ I ₃ ⁻ /CoNi ₂ S ₄ nanoribbon-CF	DSSC	15.30	0.68	0.68	7.03	[77]
Ti wire/TiO ₂ nanotube arrays/N719/I ⁻ I ₃ ⁻ /CoNi ₂ S ₄ nanorod-CF	DSSC	8.60	0.65	0.73	4.10	[77]
Ti wire/TiO ₂ nanotube arrays/N719/I ⁻ I ₃ ⁻ /Pt wire	DSSC	14.20	0.68	0.67	6.45	[77]
Ti wire/TiO ₂ nanotube arrays/N719/I ⁻ I ₃ ⁻ /Bare CF	DSSC	7.10	0.65	0.23	1.03	[77]
spring-like Ti wire/TiO ₂ nanowire array/N719/I ⁻ I ₃ ⁻ /Pt wire	DSSC	7.58	0.69	0.60	3.13	[80]
Ti wire/TiO ₂ NPs/N719/I ⁻ I ₃ ⁻ /Pt wire	DSSC	10.36	0.63	0.71	5.03	[75]
Ti wire with Microridges/TiO ₂ NPs/N719/I ⁻ I ₃ ⁻ /Pt wire	DSSC	12.34	0.69	0.74	6.29	[75]
Ti wire with microridges: nano rods/TiO ₂ NPs/N719/I ⁻ I ₃ ⁻ /Pt wire	DSSC	14.79	0.70	0.78	8.13	[75]
Ti wire with Ti nanorods/TiO ₂ NPs/N719/I ⁻ I ₃ ⁻ /Pt wire	DSSC	13.10	0.70	0.77	7.05	[75]
Ti wire/TiO ₂ nanotube array/N719/I ⁻ I ₃ ⁻ /Pt:CS-CNT composite fiber	DSSC	19.43	0.73	0.71	10.00	[83]
Ti wire/aligned titania nanotubes/N719/I ⁻ I ₃ ⁻ /Aligned CNT fibers	DSSC	8.60	0.68	0.38	2.20	[84]
Ti wire/aligned titania nanotubes/TiO ₂ NPs/P ₃ HT:PCBM/PEDOT:PSS/aligned MWCNT fiber	OPV	7.38	0.53	0.41	1.60	[92]
Ti wire/aligned titania nanotubes/P ₃ HT:PCBM/PEDOT:PSS/PSS/MWCNT sheet	OPV	6.33	0.51	0.38	1.23	[89]
CNT array/compact n-TiO ₂ /meso-TiO ₂ /CH ₃ NH ₃ PbI ₃ -xCl _x /P ₃ HT:SWNT/Ag nanowire network/CNT array	Perovskite	8.75	0.62	0.56	3.03	[95]

Table 1 (continued)

Structure	Type	J _{SC} (mA cm ⁻²)	V _{OC} (V)	FF	PCE (%)	Ref.
Stainless steel wire/compact n-TiO ₂ /meso-TiO ₂ /MAPbI ₃ /OMeTAD/CNT sheet	Perovskite	10.20	0.66	0.49	3.30	[93]
Ti wire/TiO ₂ nanotube array/CH ₃ NH ₃ PbI ₃ /CNT film	Perovskite	2.62	0.92	0.48	1.16	[100]
Ti wire/compact -TiO ₂ /meso-TiO ₂ /CH ₃ NH ₃ PbI ₃ /Spiro-OMeTAD/Ag NWs	Perovskite	11.97	0.73	0.44	3.85	[94]
Ti wire/compact -TiO ₂ /TiO ₂ nanotube array/CH ₃ NH ₃ PbI ₃ /aligned CNT sheet	Perovskite	8.90	0.85	0.48	3.6	[98]
Ti wire/compact -TiO ₂ /meso-TiO ₂ /CH ₃ NH ₃ PbI ₃ /Spiro-OMeTAD/Au	Perovskite	14.18	0.87	0.61	7.53	[101]
Ti wire/compact -TiO ₂ /meso-TiO ₂ /CH ₃ NH ₃ PbI ₃ -xCl _x /Spiro-OMeTAD/Au	Perovskite	12.32	0.71	0.61	5.35	[97]
(PEN/ITO) strip/compact -TiO ₂ /CH ₃ NH ₃ PbI ₃ /CNT sheet	Perovskite	15.90	0.91	0.66	9.49	[99]

The textiles have super flexible structures which make them capable of formability and wearability according to the users' body form. However, batteries will decrease their flexibility and increase their weight, in turn creating inconvenience in their use. Textile-based PVs are the new generation of super-flexible PVs. They could be alternative to embedded batteries inside WEDs due to their light-weight and compatibility with WEDs structures.

Smart textiles and electronic textiles (e-textiles), which emerge from the convergence and integration of textiles and electronics are also kinds of WEDs that can sense, react or adapt to the environment. The textile industry is experiencing a growing demand for high-tech materials with the increasing integration of e-textiles to create self-powered WEDs. Due to their unique formable structure, WEDs can be promisingly used in various fields such as health care, sport or military applications [65–67]. Therefore, textile-based PVs or textile solar cells are promising power harvesting candidate to enhance self-powered WEDs.

Textile solar cells can be fabricated in two ways, namely from (1) Fiber-Shaped Solar Cells (FSSCs) that are interlaced together, or (2) Planar-Shaped Solar Cells (PSSCs) that are fabricated directly on a textile substrate. The PSSC has an easier processing via direct fabrication on a prepared textile substrate, compared to FSSC. However, in contrast to PSSCs that could absorb light only from one side, FSSCs could potentially harvest sunlight from all three dimensions due to their cylindrical structure [68]. Besides, as they are light-weight and compatible with fabric weaving, their integration into textiles can be utilized for various applications [69].

Although textile solar cells are discussed in some articles [70,71], a comprehensive overview of textile solar cells, with special focus on FSSCs and PSSCs approaches towards a new generation of super-flexible solar cells, is not yet thoroughly reported in the literature. This review aims at filling this knowledge gap. FSSCs and PSSCs could potentially play a significant role in future applications, and especially for the development of battery-less self-powered WEDs. Although self-powered smart textiles and e-textiles need to simultaneously harvest and store the required electrical energy [72], the focus of this review is limited to investigate the recent research on progress of FSSCs and PSSCs which are two approaches for fabricating textile-based solar cells. We have

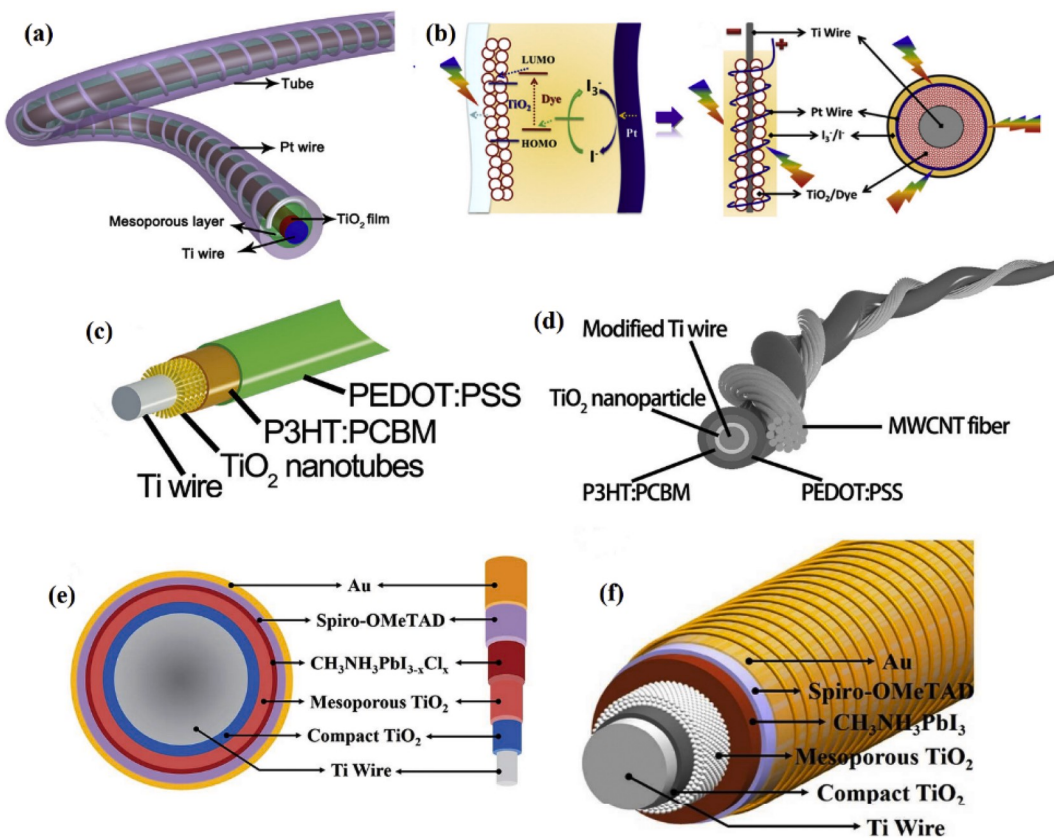


Fig. 1. Schematic representation of (a) FSDSSC, Reproduced with permission from ref. 78, Copyright 2016 Elsevier. (b) FSDSSC from different views showing the PV mechanism, Reproduced with permission from ref. 85, Copyright 2017 Elsevier. (c) FSOSC, Reproduced with permission from ref. 89, Copyright 2014 John Wiley & Sons. (d) FSOSC with multi walled carbon nanotube (MWCNT) as the top electrode, Reproduced with permission from ref. 92, Copyright 2014 John Wiley & Sons. (e) top view and cross section of a FSPSC, Reproduced with permission from ref. 97, Copyright 2016 Wiley. and (f) FSPSC with different coated PV layers, Reproduced with permission from ref. 101, Copyright 2018 Wiley.

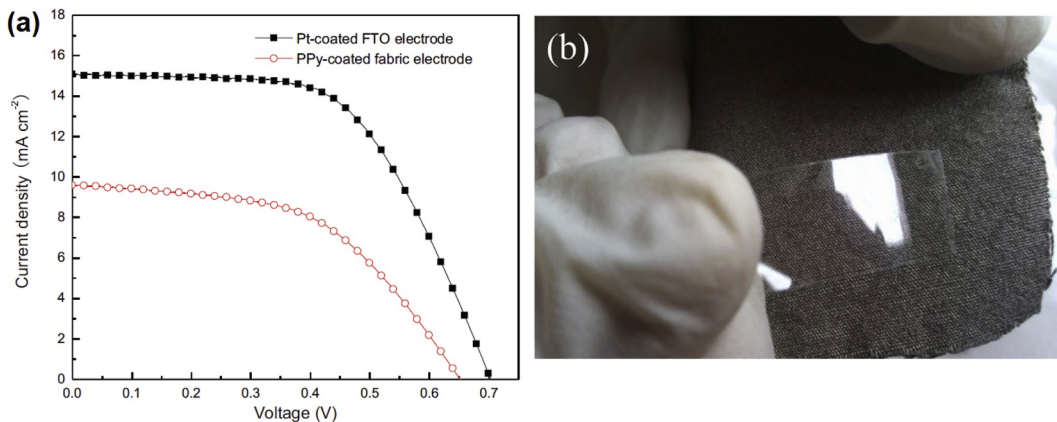


Fig. 2. (a) (J-V) characteristics of fabricated PSDSSCs with Pt-coated FTO and PPy/Ni-coated fabric counter electrodes measured under AM 1.5 illumination. (b) testing the adhesion between Ni-coated and the fabric by tape paste, Reproduced with permission from ref. 107, Copyright © 2014 Elsevier.

Table 2

PV parameters for both fabricated PSDSSCs with Pt-coated FTO and PPy/Ni-coated fabric counter electrodes, Reproduced with permission from ref. 107. Copyright © 2014 Elsevier.

Counter electrode	J _{SC} (mA cm ⁻²)	V _{OC} (mV)	FF	PCE (%)
Pt-coated FTO	15.10	704	0.58	6.16
PPy/Ni-Coted fabric	9.60	652	0.52	3.30

highlighted the relevant fabrication techniques, the advantages, and limitations together with the current challenges for Roll-to-Roll (R2R) production. Finally, the new applications and the perspectives of FSSCs and PSSCs research are discussed.

2. Structure and performance of flexible FSSCs

In order to fabricate a FSSC, the PV active layers should be coated on a cylindrical substrate (e.g. thread, metal or carbon wire, optical fiber, among others). They function either by absorbing the light from the

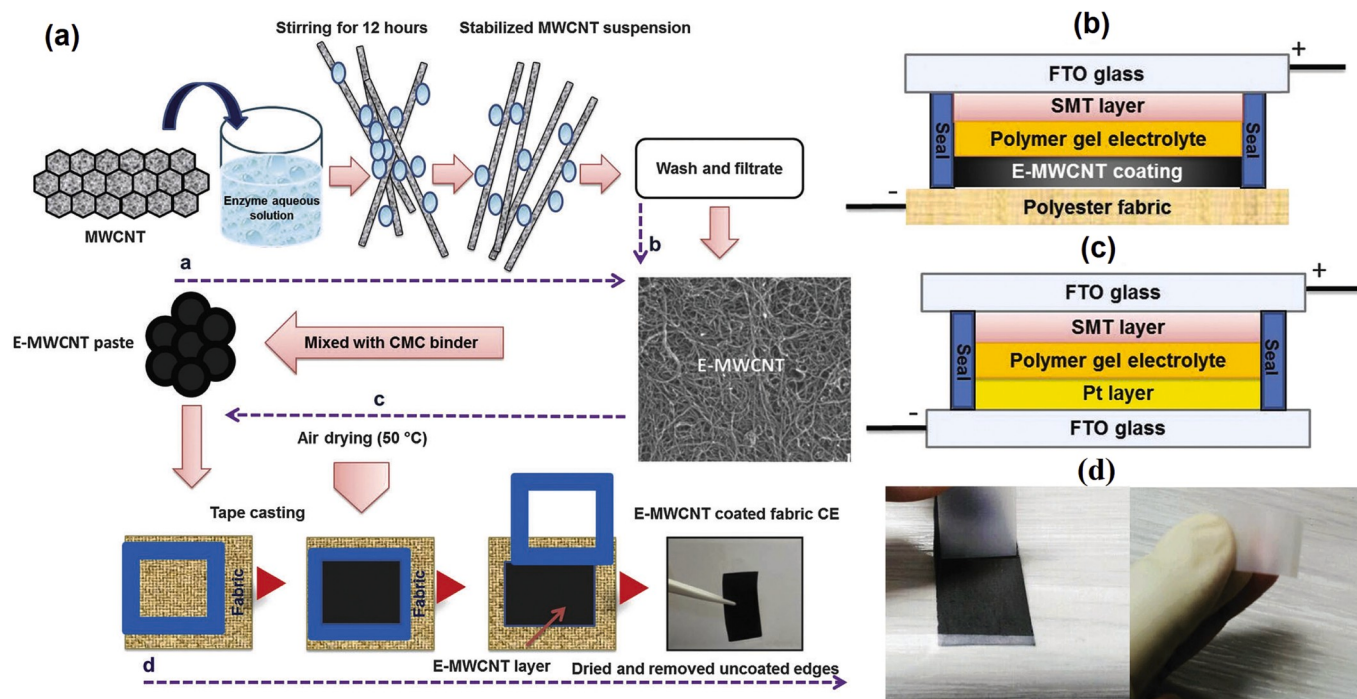


Fig. 3. (a) schematic illustration of different steps for fabrication of the PSDSSC with textile-based counter electrode (b) schematic structure of PSDSSC with textile-based counter electrode (c) schematic structure of conventional PSDSSC with Pt-coated FTO counter electrode (d) testing of the adhesion between the fabric and MWCNT layer, Reproduced with permission from ref. 108 Copyright 2015 Wiley.

external coated layer, or, in the case of an optical fiber, by in-coupling of light from the cross section of the fiber into internal PV active layers [73]. The fabricated FSSCs can subsequently be embedded inside a textile or interlaced together in order to form a textile solar cell. Recent research and development efforts have led to fabrication of Fiber-Shaped Dye-Sensitized Solar Cells (FSDSSCs) [74–88], Fiber-Shaped Organic Solar Cells (FSOSCs) [89–92], and Fiber-Shaped Perovskite Solar Cells (FSPSCs) [93–101]. Most of their structure and PV parameters, including short-circuit current density (J_{SC}), open-circuit voltage (V_{OC}), Fill Factor (FF) and PCE, are also summarized in Table 1. Fig. 1 shows a schematic drawing for the fabricated FSSCs demonstrated to date. Different types of FSSCs, the relevant structures, fabrication techniques, performance, and applications have been well studied and reported [102–106].

3. Design and fabrication of textile-based PSSCs

3.1. Textile-based dye-sensitized PSSCs (PSDSSCs)

3.1.1. Counter electrodes in PSDSSCs

In 2014 Xu et al. [107], designed and fabricated a cotton textile counter electrode for a PSDSSC, in order to replace FTO in the cells. The electrode was coated with Ni by a low temperature electroless plating technique, and was prepared with polypyrrole (PPy) as a catalytic material by dip coating followed by in situ polymerization of the pyrrole monomer on the Ni-coated textile. Fig. 2 shows the J-V characteristics of the fabricated PSDSSCs with the Pt-coated FTO and the PPy/Ni-coated fabric counter electrode. When testing the adhesion between the Ni-coated electrode and fabric demonstrated relatively high resilience to delamination effects was demonstrated. As shown in Table 2, the PCE, fill factor, J_{SC} and V_{OC} of the fabricated PSDSSC with the textile-based counter electrode are all lower than for the conventional DSSC with Pt-coated FTO counter electrode, dropping almost 50% in PCE when moving to a fabric electrode material. Still, this work is relevant because it demonstrated a possible route for development of a textile-based counter electrodes for PSDSSCs.

Arbab et al. [108], fabricated another textile counter electrode with polyester fabrics in 2015. They demonstrated the coating of a layer of multiwalled carbon nanotubes (MWCNT) layer with different thicknesses, and various MWCNT sizes. Interestingly, different enzymes were used on the polyester fabric, via a simple tape casting technique, in order to decrease the agglomeration of the MWCNTs without perturbing their electronic properties. Fig. 3(a–c) depict the most relevant different fabrication steps and the schematic illustration of different layers in the fabricated PSDSSC. Fig. 3(d) also shows that the adhesion between the coated MWCNTs and fabric was strong, as proven by a scotch tape test. The device characterization, Fig. 4 and Table 3, showed that, although the efficiency of the fabricated PSDSSC with the textile counter electrodes was lower compared to the reference PSDSSC with the standard Pt-FTO coated glass counter electrodes, yet the PSDSSC with the flexible counter electrode demonstrate quite reasonable PCE values of 5.7%, due to an almost fully retained V_{OC} and FF.

In a similar research work, Sahito et al. [109], fabricated a flexible and Highly Conductive Graphene-Coated Cotton Fabric (HC-GCF), and employed it as a counter electrode in PSDSSCs. In order to develop a positively charged surface the graphene oxide nanosheets were coated by cationization of a cotton fabric, followed by soaking of the cotton fabric in graphene oxide nanosheet (GON) dispersions. A chemical reduction method was used to turn the graphene oxide into graphene nanosheets, using a hydrazine monohydrate solution. The surface resistance of the highly conductive graphene coated cotton fabric was $7 \Omega \text{ sq}^{-1}$. A power conversion efficiency (PCE) of 6.93% was obtained in comparison to 8.44% for the DSSC with Pt-FTO counter electrodes. The fabrication process and device performance results are shown in Fig. 5 and Table 4.

In 2016 Arbab et al. [110], fabricated a textile fabric counter electrode in PSDSSCs based on activated charcoal doped multi walled carbon nanotubes (AC doped MWCNT), which was printed on a 100% polyester woven fabric by doctor blading technique (Fig. 6). Three types of activated charcoal coal (composite A), coconut shell (composite B) and pine tree (composite C) were used with different wt% of AC in order to fabricate the AC doped MWCNT. Results showed that the pine tree

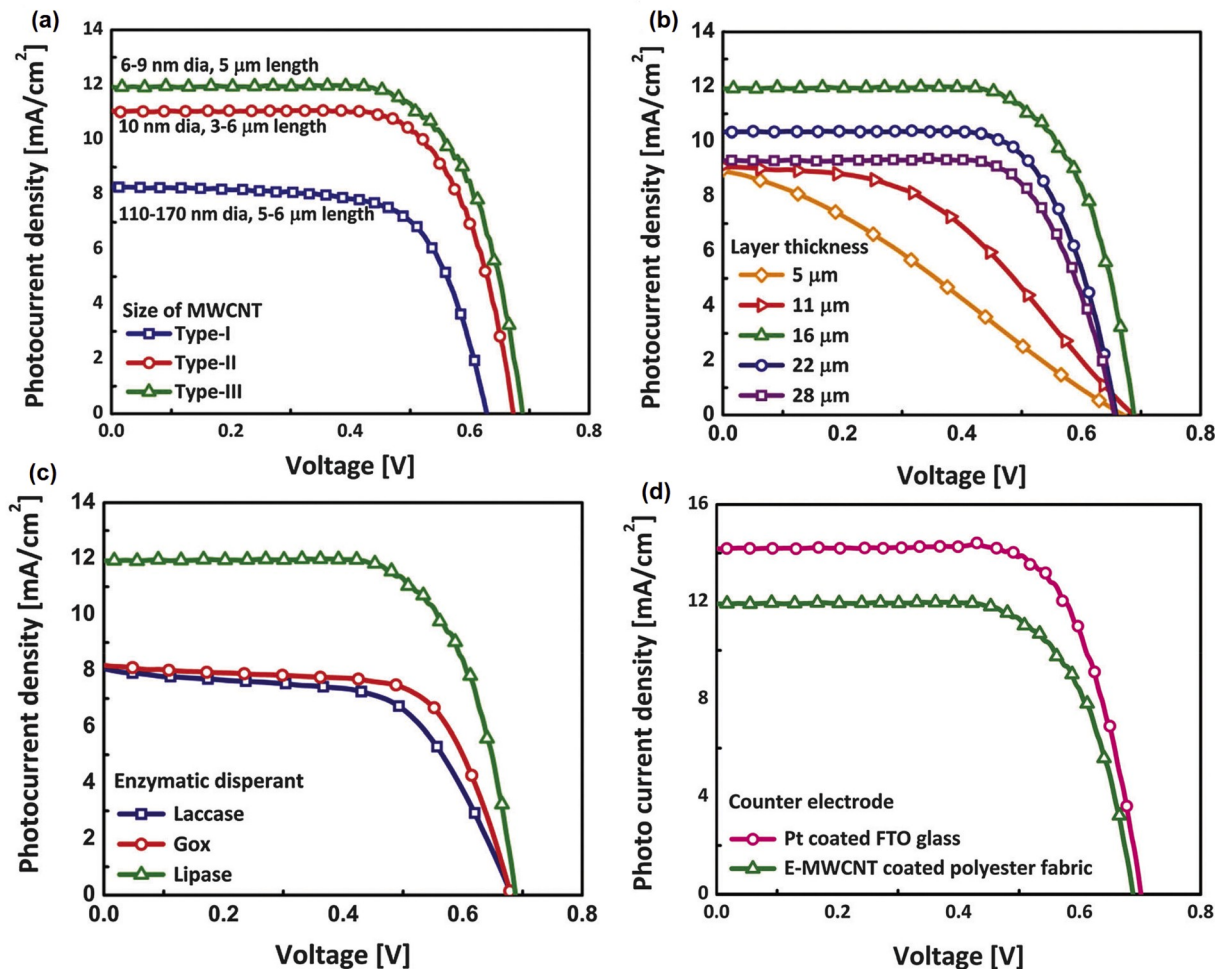


Fig. 4. J-V characteristics of the fabricated PSDSSCs using (a) different size of MWCNT (b) different layer thickness of E-MWCNT (c) different enzymes and (d) the comparison between the conventional Pt coated FTO glass and the textile MWCNT coted counter electrodes, Reproduced with permission from ref. 108 Copyright 2015 Wiley.

composite (composite C) with 0.8 wt% of AC into the MWCNT dispersions reached the highest PCE (7.29%) for the textile fabric counter electrodes (Fig. 7(a and b), Tables (5 and 6). Fig. 7(c) and Table 7 depict the comparision between PV parameters of PSDSSCs fabricated with Pt and carbon fabric counter electrodes.

Memon et al. [111], fabricated textile-based counter electrodes from cotton, polyester, and linen fibers using highly photo- and electro-catalytic activated carbon composites made from highly conductive functionalized Multi-walled Carbon Nanotubes with Mesoporous Activated Charcoal (M-AC/MCNT). The PCE of the fabricated PSDSSCs with the textile based counter electrodes based on polyester, cotton and linen was 6.26%, 6.06% and 5.80% respectively, which is comparable to the 7.26% delivered by the reference device with Pt-coated counter electrode reference.

3.1.2. Insertion of DSSCs into textiles

In 2015 Yun et al. [112], introduced in 2015 a new approach for the incorporation of DSSC electrodes into textiles during the weaving process of making the textile. In this structure, the TiO₂ Dye-Loaded Porous (DLP) was coated on a metal ribbon, which was used as the photoanode. Pt NanoParticle-Loaded Carbon Yarn (Pt-NPLCY) was used as the counter electrode. The photoanode and counter electrode was weaved together as the warp or weft. Finally, the fabricated DSSC textile solar cell was sewn into a garment. As shown in Fig. 8(a-c) in details, the Pt loaded carbon yarn was weaved as a weft, the counter electrode and the dye loaded TiO₂ on a stainless steel ribbon having the photoanode were

weaved as warps in the bottom and top of the fabric, Nylon filaments were weaved as warps in order to support the photoanode metal ribbon and maintaining the space between the photoanode and the counter electrode for preventing short circuits until filling the electrolyte. The PCE of the inserted DSSC in the textile was 2.63%, having a J_{SC} of 5.78 mA/cm⁻², a V_{OC} of 0.725 V, and a fill factor of 0.63 (Fig. 8(d)).

Although this presents an innovative idea for weaving of DSSC devices into a textile structure, the fabricated textile solar cell was not still completely flexible due to the insertion of the metal ribbon and metal wires as different parts of the DSSC.

3.1.3. Coating DSSC layers on a textile

Opwis et al. [113], fabricated a textile-based PSDSSC on a woven fabric from glass-fibers. At first, they covered a glass-fiber fabric with a thin polyamide (PA) film made from R2R processing, in order to prepare a uniform and smooth surface for coating of the PV layers (Fig. 9(a and b)). Afterwards, a titanium layer was made by electron beam or sputter deposition, followed by screen printing of titanium dioxide and curing at

Table 3

PV parameters of fabricated PSDSSCs with different counter electrodes, Reproduced with permission from ref. 108 Copyright 2015 Wiley.

Counter electrode	J_{SC} (mA cm ⁻²)	V_{OC} (mV)	FF	PCE (%)
Pt/FTO	14.18	701	0.72	7.16
E-MWCNT/fabric	11.92	688	0.69	5.69

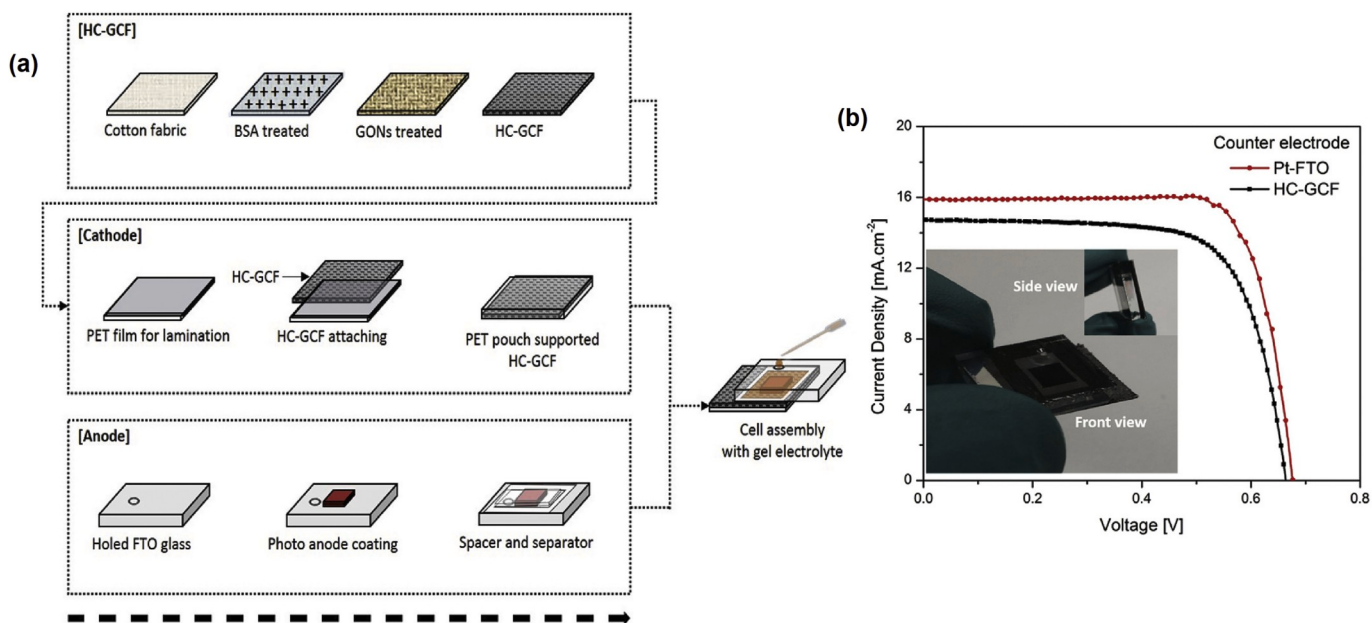


Fig. 5. (a) Schematic explanation of the different fabrication steps used for developing the PSDSSC with textile-based counter electrodes (b) J-V curves of Pt and HC-GCF counter electrode based PSDSSCs, Reproduced with permission from ref. 109 Copyright 2016 Elsevier.

Table 4

PV characteristic of the Pt and HC-GCF counter electrode based PSDSSCs, Reproduced with permission from ref. 109 Copyright 2016 Elsevier.

Counter electrode	J_{SC} (mA cm^{-2})	V_{OC} (mV)	FF	PCE (%)
Pt - FTO	15.88	670	0.79	8.44
HC-CGF	14.75	660	0.71	6.93

500°C for 5 min. The active layer was synthesized by ruthenium-based dyes. After adding the electrolyte, a thin film of PEN + ITO was coated by the catalyst layer of Pt from the chemical reduction of H₂PtCl₆ at room temperature, which was used as the counter electrode on the previous layers. Finally, the fabricated PSDSSC (glass-fiber fabric + PA layer + Ti + dye-sensitized TiO₂ + electrolyte + PEN + ITO + Pt) was sealed by special epoxy thermoplastic foils (Fig. 9(c and d)). The best fabricated textile-based PSDSSC worked with 1.83% efficiency (Fig. 9(e), Table 8). Although a novel and innovative prototype of a textile-based PSDSSC was fabricated via this approach, it was carried out on a woven glass-fiber that is more expensive than conventional woven

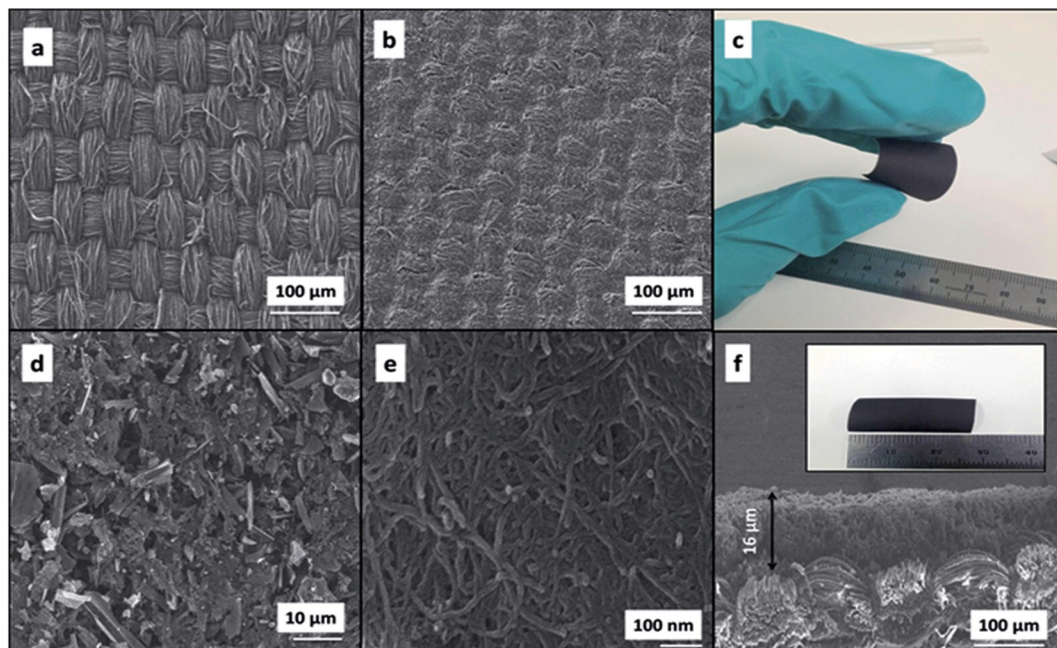


Fig. 6. FE-SEM images of (a) uncoated polyester fabric (b) AC doped MWCNT coated fabric (c) image of the flexible carbon fabric (d) Low magnification FE-SEM image of the AC doped MWCNT (e) High magnification FE-SEM image of the AC doped MWCNT (f) Cross-sectional FE-SEM image of the carbon fabric composite with the image of the carbon fabric composite, Reproduced with permission from ref. 110 Copyright 2016 Wiley.

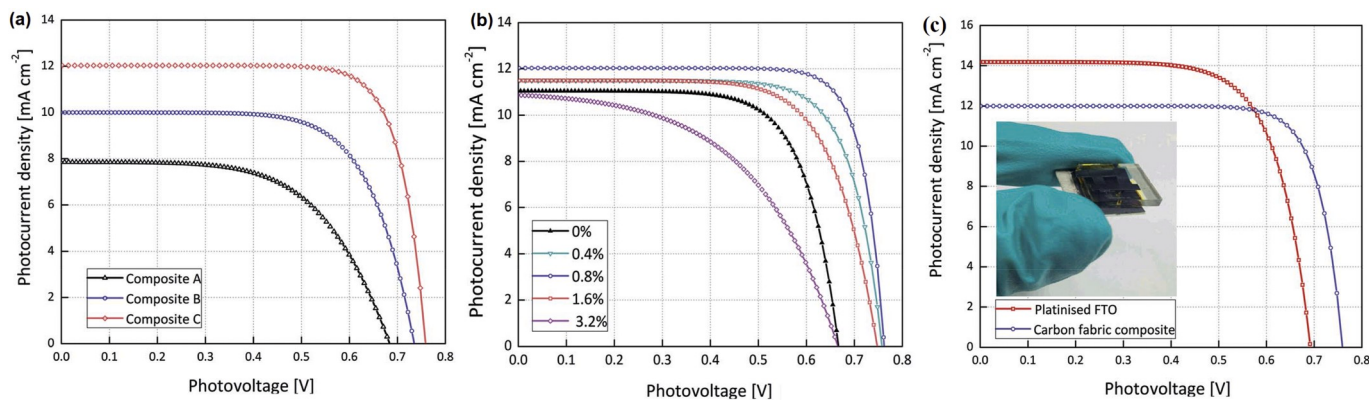


Fig. 7. J-V curves of fabricated PSDSSCs based on (a) three types (composite A, B and C) of carbon fabric composites counter electrodes and (b) different wt% of charcoal on PV performance (c) the comparison between I-V curves of PSDSSCs fabricated with Pt and carbon fabric CEs, Reproduced with permission from ref. 110 Copyright 2016 Wiley.

Table 5

PV performance of PSDSSCs fabricated with different carbon fabric composites, Reproduced with permission from ref. 110 Copyright 2016 Wiley.

Type of composite	J_{SC} (mA cm^{-2})	V_{OC} (mV)	FF	PCE (%)
Composite A	8.06	681	0.60	3.31
Composite B	10.09	735	0.68	5.03
Composite C	11.50	743	0.70	5.97

fabrics. The fabrication process was also done at high temperatures (500 °C), which finally unavoidably increases the fabrication costs. However, such development also puts emphasis on the need for smooth and uniform planar layers, which yielded decent performance results in this work.

3.2. Textile-based organic PV (OPV) PSSCs

In 2014, Lee et al. [114], introduced a textile-based OPV as a stitchable power source. They used an ITO coated flexible film as bottom electrode, Zinc Oxide (ZnO) as the electron transport layer, spin-coated P3HT:PCBM as the bulk heterojunction photoactive layer, molybdenum trioxide (MoO_3) deposited by thermal evaporation as the hole transport layer, and finally a gold textile electrode placed as the top electrode by physical lamination onto the MoO_3 layer. The fabricated solar cell was integrated into a textile providing a PCE of 1.79% for the textile-based solar cell, and 2.97% for the reference organic solar cell with a thermally evaporated silver top electrode. Although this work demonstrated a novel idea for fabrication of a textile-based OPV device, the PCE remained low due to the purely physical connection between the gold textile electrode and the hole transporting layer. In future, a cheaper method for developing the electrode connection from R2R production would be needed, in order to demonstrate the further viability of this approach.

Kylberg et al. [115], introduced a flexible and transparent textile-based electrode made of woven polymer and metal fibers. The open spaces between the polymer and metal fibers were filled with a transparent polymer fabricated by immersing the woven textile in the liquid polymer and using doctor blading. Subsequently, the transparent polymer was cured and stabilized with UV light. A layer of PEDOT:PSS was coated on the prepared textile by doctor blading, and an active layer of poly(3-hexylthiophene) (P3HT)/phenyl-C61-butyric acid methyl ester (PCBM) was spin coated on the poly(3,4-ethylenedioxythiophene) polystyrene sulfonate (PEDOT:PSS) layer. Finally, an aluminum layer was thermally evaporated as the back contact (Fig. 10). Table 9 shows the effect of the PEDOT:PSS thickness on the performance of the fabricated solar cell using the woven textile electrodes, as well as reference

Table 6

PV performance of PSDSSCs fabricated with carbon fabric composites of different wt% of activated carbon (pine type), Reproduced with permission from ref. 110 Copyright 2016 Wiley.

wt% of carbon	J_{SC} (mA cm^{-2})	V_{OC} (mV)	FF	PCE (%)
0	11.05	673	0.70	5.24
0.4	11.52	769	0.74	6.56
0.8	12.03	766	0.79	7.29
1.6	11.50	743	0.70	5.97
3.2	11.03	665	0.49	3.61

solar cells based on FTO coated glass. A decreasing PEDOT:PSS thickness resulted in enhanced J_{SC} values due to an increased transmittance of the transparent electrode. Bending tests for evaluating the mechanical stability of the solar fabric with bending radius 0.6 cm were carried out, and no decrease in conductivity after a 100 bending cycles was reported.

In 2015 Steim et al. [116], used a conductive fabric made of poly(ethylene 2,6 naphthalate) (PEN) with Ag coated metallic woven wires as the top electrode in an organic solar cell. Aluminum-doped zinc oxide (AZO) and Ag (AZO/Ag/AZO) was coated on a polyethylene terephthalate (PET) foil from a sputtering technique. The transparent bottom electrodes had sheet resistance of $10 \Omega \text{sq}^{-1}$. Different layers including P3HT:PCBM, PEDOT:PSS HTL, and PEDOT:PSS F ET were coated on the substrate, respectively, by doctor blade technique, followed by lamination onto wet PEDOT:PSS F ET films using manually applied pressure. After heating at 60 °C, the PEDOT:PSS F ET strongly adhered to the fabric and the contact between the metal wires and the OPV cell was formed. Finally, the OPV was encapsulated between glasses with an epoxy based liquid adhesive. Fig. 11(a) shows the schematic structure of fabricated OPV with the fabric as a top electrode. Fig. 11(b) shows the J-V curves for fabricated and encapsulated solar cells, which are illuminated from both the fabric and AZO/Ag/AZO side. Results showed that for illumination from the fabric top electrode side, J_{SC} was 5 mA/cm^2 , the V_{OC} 0.57 V, and FF 53%, thus resulting in a PCE of 1.5%. For the illumination through the AZO/Ag/AZO bottom electrode side, a similar PCE of 1.6% was obtained, with slightly higher J_{SC} values due to the improved transparency. Although the top electrode inside this solar cell was fabric-based, the main substrate was a flexible PET sheet

Table 7

The comparison between PV parameters of PSDSSCs fabricated with Pt and carbon fabric CEs, Reproduced with permission from ref. 110 Copyright 2016 Wiley.

CEs	J_{SC} (mA cm^{-2})	V_{OC} (mV)	FF	PCE (%)
Platinized FTO	14.18	701	0.72	7.16
Carbon fabric	12.03	766	0.79	7.29

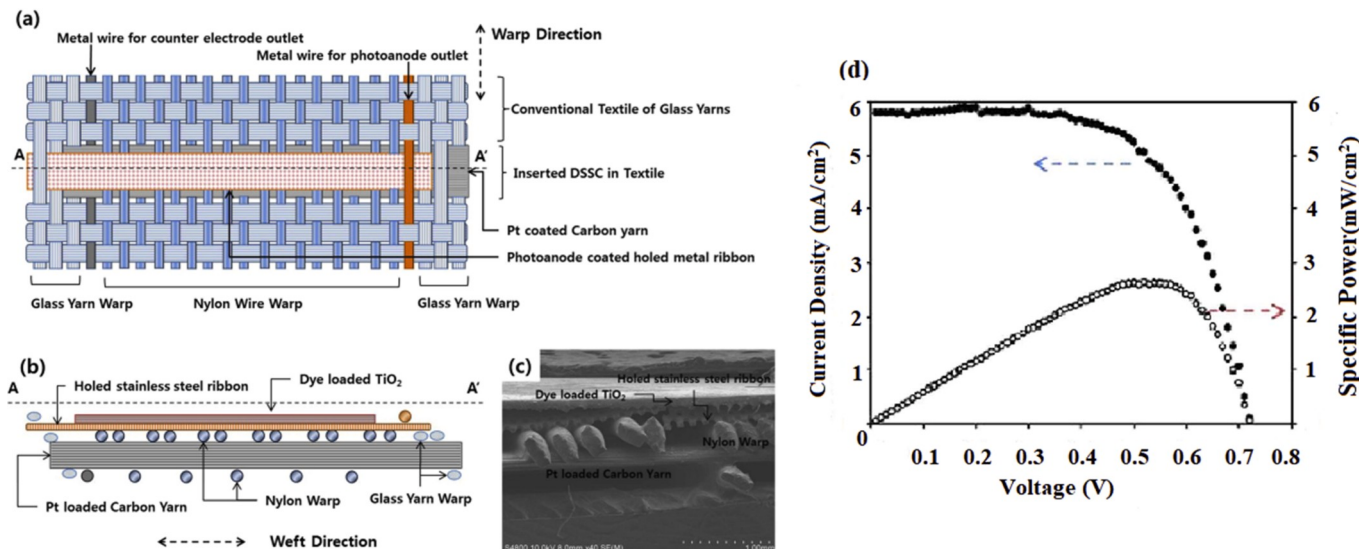


Fig. 8. Schematic illustration of the structure of the inserted DSSC into the textile from the (a) top view (b) cross section view and (c) cross sectional SEM image (d) PV characteristics curves of inserted DSSC into the textile [112].

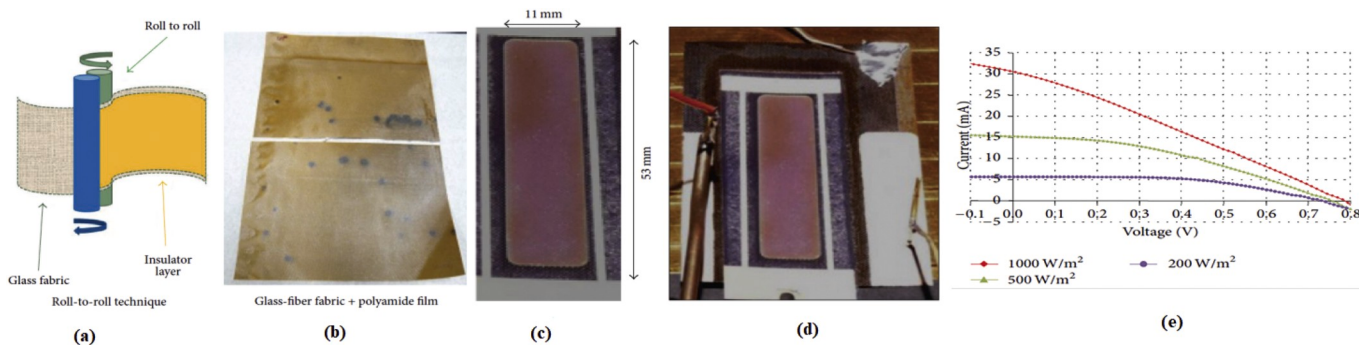


Fig. 9. The images of (a) schematic illustration of R2R coating technique (b) coated glass fiber fabric by PA (c) prepared textile based PSDSSC (d) 4-point configuration used for J-V characterization (e) I-V curves of fabricated textile based PSDSSC at different irradiance level [113].

Table 8

PV parameters of fabricated textile based PSDSSC at different irradiance level [113].

Irradiance (W/m ²)	J _{SC} (mA cm ⁻²)	V _{OC} (mV)	FF	PCE (%)
1000	5.10	790	0.27	1.10
500	2.55	750	0.39	1.51
200	0.95	710	0.54	1.83

that is not as flexible as fabrics and textiles.

In 2015 Arumugam et al. [117], fabricated an organic solar cell on a 65/35 polyester cotton woven fabric as a textile substrate. Polyurethane based interface paste was initially coated on the fabric substrate by a screen printing technique, in order to decrease the roughness and smoothening of the fabric surface. A suspension of metallic AgNW in isopropyl alcohol (IPA) was used for spray coating of AgNW as the bottom electrode. An electron transport layer of ZnO-NP with an average particle size <35 nm that had been dispersed (40 wt%) in ethanol was coated on the bottom electrode by spray coating technique. A blend of regioregular poly(3-hexylthiophene) (P3HT):Indene-fullerene C60 bisadduct (ICBA), dissolved in 1,2-dichlorobenzene was used as the photoactive layer on the electron transport layer. Then a layer of PEDOT:PSS dispersion in water was coated on the active layer as the HTL. At last, an AgNW was coated on the hole transport layer as the top electrode (Fig. 12). Fig. 13 shows different SEM pictures from different

aspects of the fabricated textile solar cells. Fig. 14 represent J-V curves of the fabricated textile solar cells and the same PV structure on a glass substrate developed by the spray coating technique. As shown in Table 10, the reference solar cells on glass showed an expected higher performance than the textile solar cells, partially due to uniform coverage of the PEDOT:PSS layer and the smoother surface of the P3HT:ICBA layer. However, the fill factors of the reference devices are quite low. The approach was innovative for the fabrication of a textile solar cell that could potentially be embedded in wearable and formable devices, however, the device efficiency needs to be further boosted. This works also highlights how the development of the bottom and top electrode is one of the main challenges in this research field.

Recently, Li et al. [118], have fabricated a textile OPV by printing and spray coating technique. They used woven 65/35 polyester cotton fabric as the textile substrate. First, they coated three interface layers on the textile substrate with overall thickness of 250 μm in order to reduce the roughness of textile substrate for achieving a smooth substrate. Then, they coated Ag electrode, ZnO layer, active layer, PEDOT:PSS layer, and Ag nanowire layer by spray coating technique. The fabricated textile OPV has V_{oc} of 0.5 V, J_{SC} of 3.44 (mA/cm²), FF of 0.24 and PCE of 0.4%. Fabricated textile solar cells were encapsulated for protecting them from air and improving their stability. Results showed that un-encapsulated textile solar cells could not survive more than 2 days while encapsulated textile solar cells could work during 30 days with

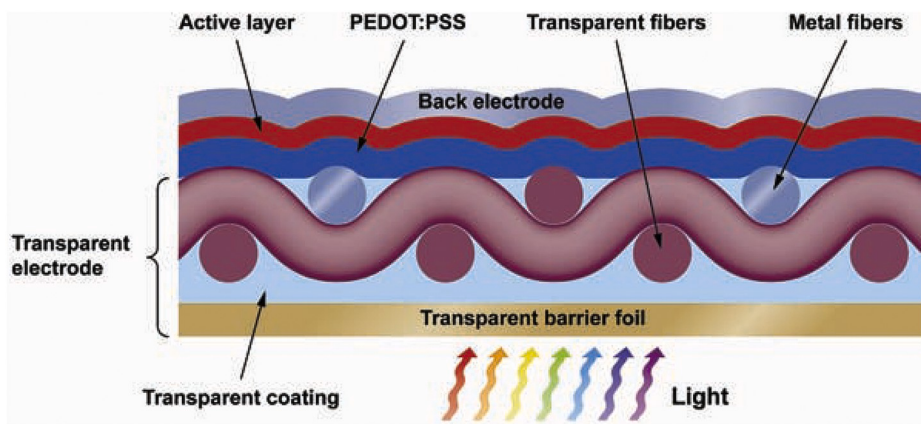


Fig. 10. Cross sectional schematic view of fabricated OPV with transparent textile based top electrode, Reproduced with permission from ref. 115 Copyright 2010 John Wiley & Sons.

Table 9

PV performance parameters for textile based and ITO coated glass electrodes with different thickness of PEDOT:PSS, Reproduced with permission from ref. 115 Copyright 2010 John Wiley & Sons.

Substrate	J_{SC} (mA cm^{-2})	V_{OC} (V)	FF	PCE (%)
Fabric (1.6 μm PEDOT:PSS)	8.50	0.56	0.46	2.2 \pm 0.2
Fabric (1 μm PEDOT:PSS)	11.50	0.52	0.37	2.2 \pm 0.2
Glass-ITO (1.6 μm PEDOT:PSS)	9.40	0.53	0.48	2.4 \pm 0.1
Glass-ITO (spin-cast PEDOT:PSS)	10.90	0.56	0.52	3.2 \pm 0.1

100% PCE, during 30 to 60 days with 75% PCE, and after 60 days with less than 25% PCE.

3.3. Textile-based perovskite (PSPSCs)

In 2017, Lam et al. [119], integrated a washable and flexible perovskite solar cell on a textile. SnO_2 was electrodeposited on the flexible ITO coated PEN substrate as the electron transporting layer (ETL). A thin layer of PCBM was spin coated on the SnO_2 layer in order to decrease the roughness of the SnO_2 coated layer for improved electron transport. The perovskite layer of MAPbI_3 and HTL of Spiro-OMETAD were spin coated on the previous layers. Finally, a gold top electrode was thermally evaporated on the HTL layer. The fabricated solar cell was encapsulated by a 3 MTM acrylic elastomer and adhered to the textile

(Fig. 15). This textile-based flexible perovskite solar cell was characterized immediately after development and after immersion in the water (Fig. 16(a and b)) and Table 11). As the J-V in Fig. 16(c) shows, the performance of the fabricated textile solar cell was nearly stable during the water immersion cycles, demonstrating the high barrier quality in their solution. Fig. 16(d and e) show pictures of fabricated textile-based PSPSC and its application for lighting up an integrated LED inside the textile.

Although this work demonstrated the development of a textile-based perovskite solar cell with good stability properties for the addressed application, it still showed limited flexibility, as the standard perovskite cell stack was integrated directly onto the textile. Therefore, the integrated solar cell cannot be formed and folded, highlighting the remaining limitations for achieving complete device flexibility.

In 2018, Jung et al. [120], could fabricate a textile-based PSPSCs on a Polyester/satin textile substrate. They coated a thin layer of polyurethane (PU) by a paper transfer lamination method on the textile in order to have an even and smoother textile substrate surface for solution-processing. After that, they coated an inverted PV architecture PEDOT:PSS by scalable printing technique as the anode instead of ITO or FTO and doctor blading 0.5 wt% single-walled carbon nanotubes (SWCNTs) in PEDOT:PSS in order to improving the conductivity/printing a low conductivity PEDOT:PSS HTL/printing perovskite absorber layer of $\text{CH}_3\text{NH}_3\text{PbI}_3$ /printing PCBM by bar coating technique as the Electron Transport Layer (ETL). Finally, they thermally

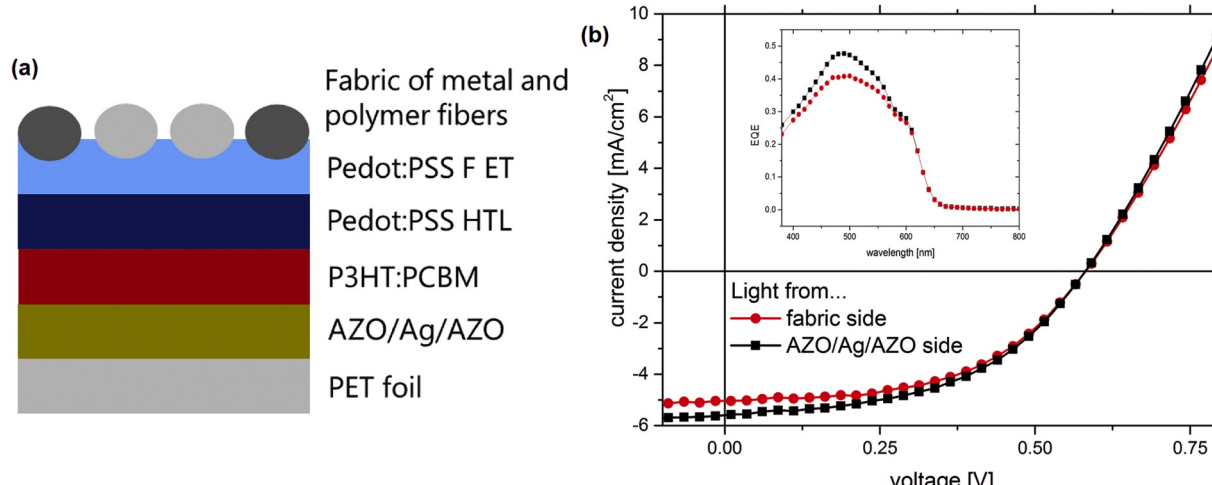


Fig. 11. (a) Schematic image of the structure of fabricated top electrode fabric based OPV (b) J-V characteristics for the fabric based OPV with illuminated from both the fabric side and AZO/Ag/AZO side, Reproduced with permission from ref. 116 Copyright 2015 AIP Publishing.

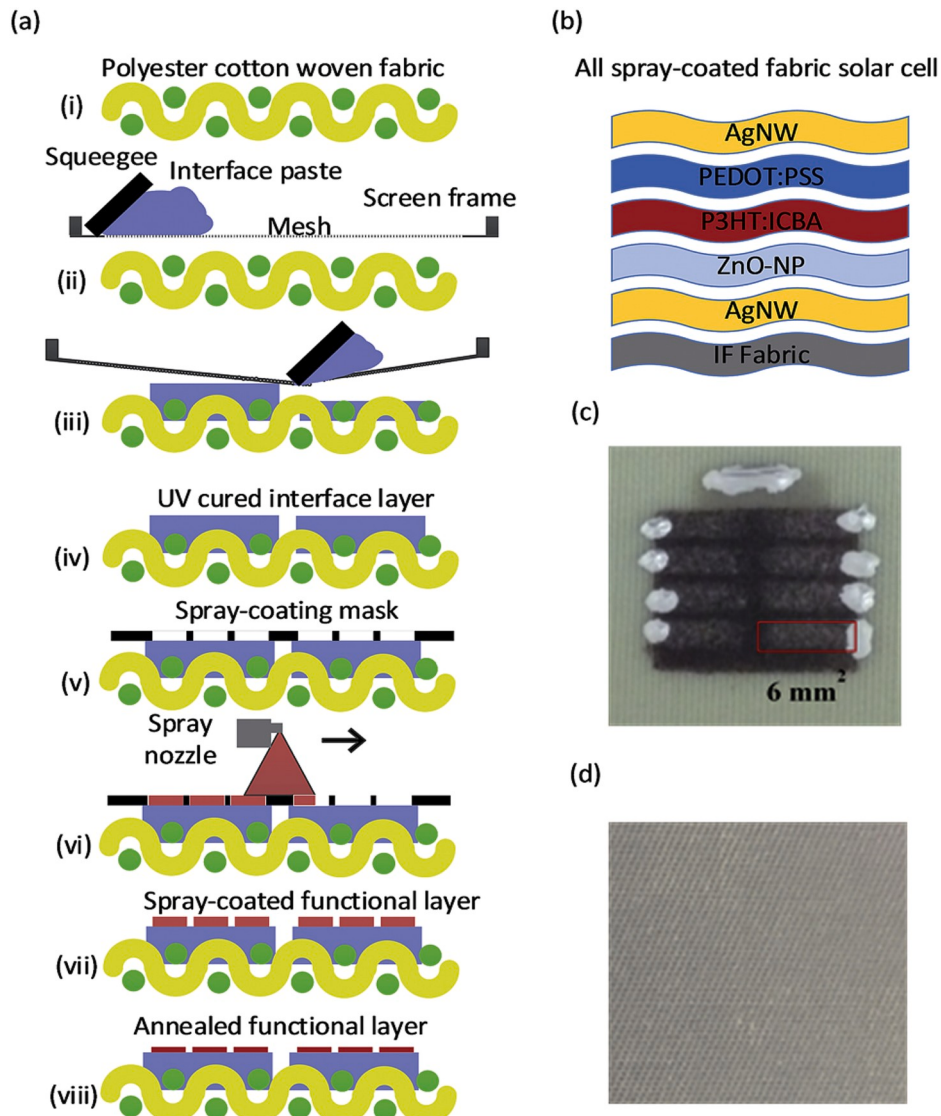


Fig. 12. Schematic illustration of (a) fabrication process of OPV textile based (b) cross sectional view of different PV layers (c) image of the fabricated OPV from the front side (d) image of the fabricated OPV from the back side, Reproduced with permission from ref. 117 Copyright 2016 Wiley.

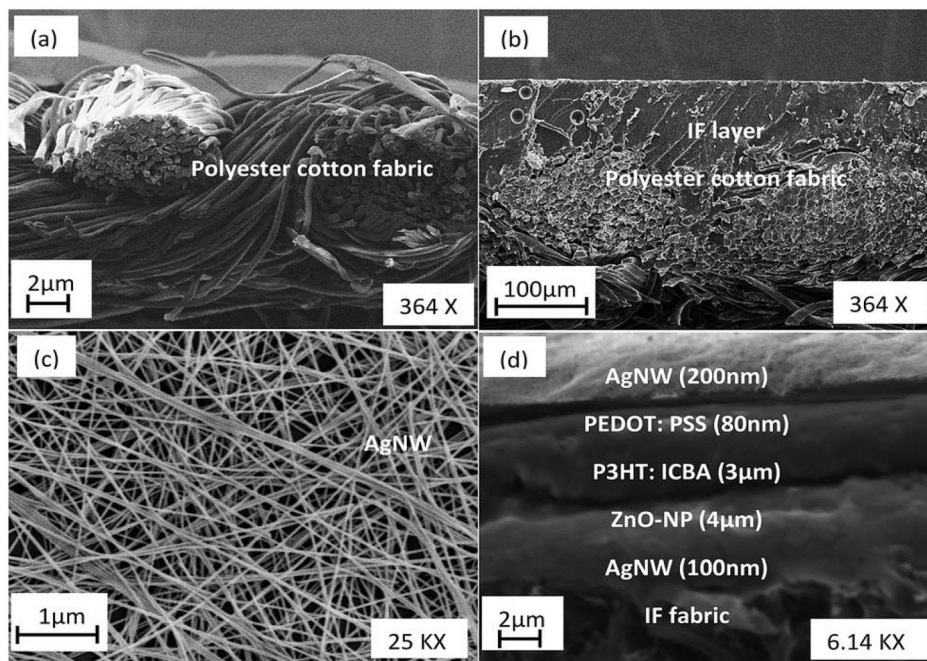


Fig. 13. (a) cross section SEM image of woven Polyester (65)/Cotton (35) fabric substrate (b) SEM image of the coated interface layer on the fabric (c) FE-SEM image of the spray coated AgNW on the fabric substrate as the bottom electrode (d) SEM image (cross section view) of different PV layers, Reproduced with permission from ref. 117 Copyright 2016 Wiley.

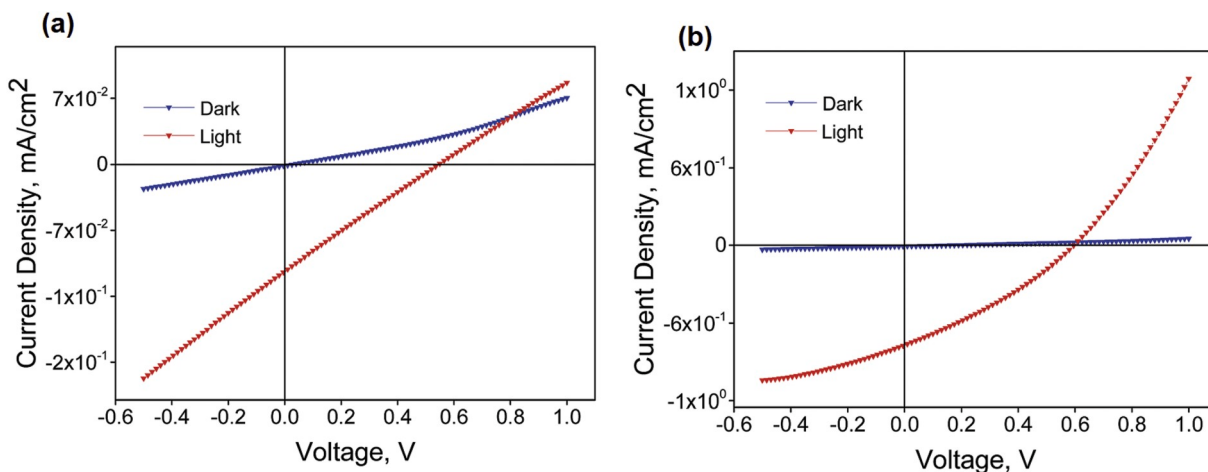


Fig. 14. J-V curves of the OPV devices fabricated by spray coating technique on (a) fabric substrate (type 1) (b) glass substrate (type 2), Reproduced with permission from ref. 117 Copyright 2016 Wiley.

Table 10

PV parameters of fabricated OPV on fabric and glass substrates, Reproduced with permission from ref. 117 Copyright 2016 Wiley.

Devices	Device structure	J_{SC} (mA cm $^{-2}$)	V_{OC} (V)	FF	PCE (%)
Type 1	IF fabric/AgNW/ZnO-NP/P ₃ HT:ICBA/PEDOT:PSS/AgNW	0.11	0.55	0.24	0.01
Type 2	Glass/AgNW/ZnO-NP/P ₃ HT:ICBA/PEDOT:PSS/AgNW	0.76	0.61	0.30	0.14
Type 3	IF fabric/pressed AgNW/ZnO-NP/P ₃ HT:ICBA/PEDOT:PSS/AgNW	0.26	0.41	0.25	0.02

evaporated 8 nm of Ag as transparent top-electrode. [Fig. 17](#) shows a schematic illustration for the whole of perovskite PSSCs textile-based structure and a cross-sectional SEM picture of PU coated textile substrate. The champion device, which was achieved in 600 nm perovskite thickness, led to PCE of 5.17%, V_{OC} of 0.82V, J_{SC} of 12.69 mA cm $^{-2}$, and FF of 0.5. [Table 12](#) shows PV parameters of fabricated perovskite textile-based with different thicknesses of perovskite layer.

3.4. Comparison between different types of PSSCs textile-based

In most of the reported studies on fabricated textile-based PSDSSCs, researchers have successfully demonstrated the development and fabrication of DSSC from a flexible textile-based counter electrode, which are important steps towards the development of textile-based PVs. However, as the DSSC is still using glass-based working electrodes in the mentioned works, the complete devices are not flexible,

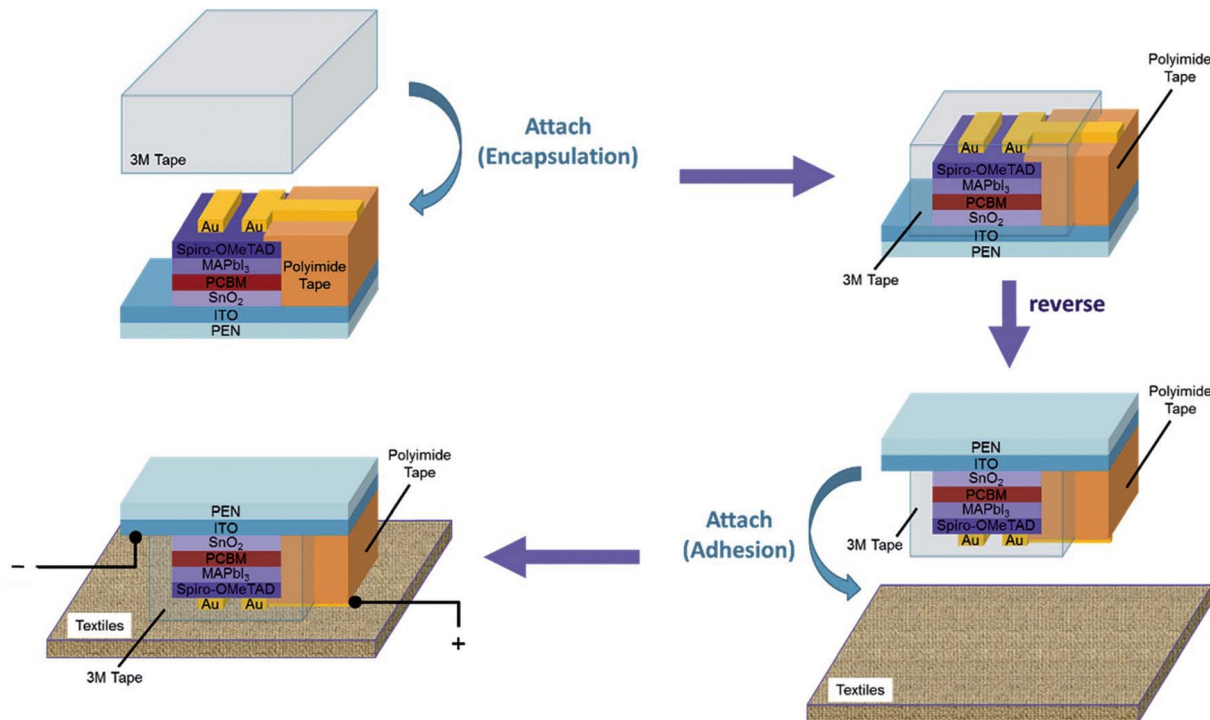


Fig. 15. Schematic illustration of the fabrication process of the textile-based flexible PSPSC [119].

Table 11
PV parameters of textile-based PSCs using SnO_2 ETL and SnO_2/PCBM ETL [119].

Electron-transporting layer		J_{SC} (mA cm^{-2})	V_{OC} (V)	FF	PCE (%)
SnO_2 (0.8 sun) ^a	F	-13.47	1.03	0.31	5.4
SnO_2 (0.8 sun) ^a	R	-12.16	1.02	0.41	6.3
SnO_2/PCBM (0.8 sun)	F	-17.07	1.08	0.63	14.5
SnO_2/PCBM (0.8 sun)	R	-17.05	1.06	0.65	14.8
SnO_2/PCBM (1 sun)	F	-20.90	1.07	0.62	13.9
SnO_2/PCBM (1 sun)	R	-20.53	1.06	0.66	14.3

F: forward-bias sweep (-0.1 V–1.2 V); R: reverse-bias sweep (1.2V to -0.1V). Time of electrodeposition for SnO_2 : 120 s.

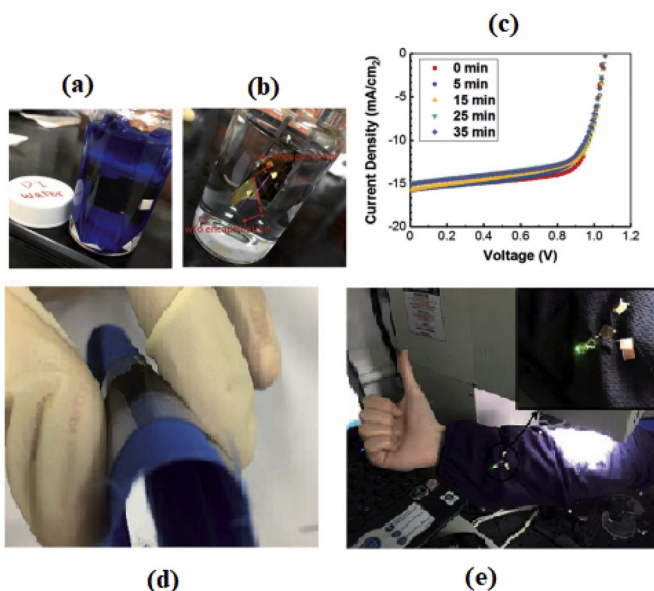


Fig. 16. Image of (a) the textile-based PSPSC immersed in water (b) fabricated textile-based PSPSC with and without encapsulation while immersing in water (c) J-V curves of the textile-based PSPSCs for different immersion times in the water (d) fabricated flexible textile-based PSPSC (e) a commercial LED lit up by the fabricated textile-based flexible PSCs under 0.8 sun illumination [119].

and thus they are just a first step of a longer development route for textile PV devices. Fabricated textile-based OPV PSSCs are flexible enough for wearable applications, but they still perform poorly in terms of PCE and stability. In literature, there are fewer studies for textile-based perovskite PSSCs compared to those on other types of textile-based PSSCs, being perovskite a younger PV technology. However, the reported works demonstrate that perovskite solar cells are more promising than other solar cells for developing textile-based PSSCs due to their more compatible structure with flexible substrates, higher efficiency and stability, and at the same time easier solution-processable fabrication process. The textile-based PSSCs structures and their PV parameters are summarized in Table 13.

4. Summary, challenges and outlook

In this review, various research work on textile solar cells have been introduced and compared in this paper, looking into both FSSCs and textile-based PSSCs developed within the DSSC, OPV, and perovskite solar cell technologies. The high flexibility of FSSCs is a unique advantage that make them capable for application in wearable power harvesting applications. Despite the promising progress on the device performance of FSSCs, the fabrication of a FSSC is a cost consuming process that needs special techniques due to their three dimensions and the cylindrical shape of the substrate. Furthermore, weaving of the FSSC

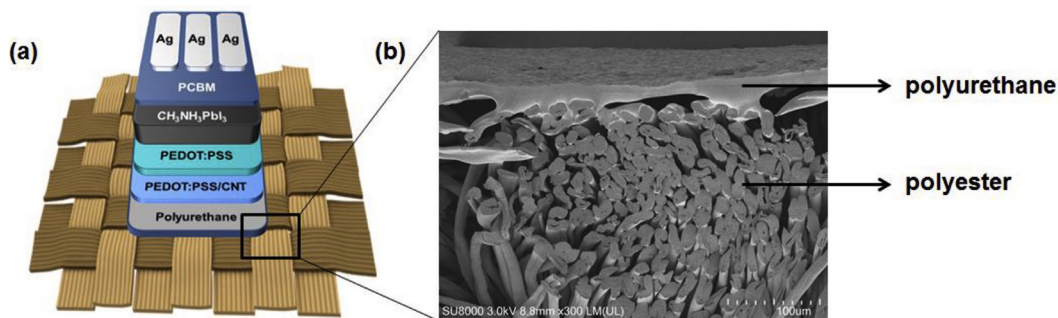


Fig. 17. (a) Schematic illustration of textile-based PSPSCs structure (b) SEM image of the PU coated textile substrate, Reproduced with permission from ref. 120 Copyright 2018 Elsevier.

Table 12

PV parameters of textile-based PSPSCs with different thicknesses of perovskite layer, Reproduced with permission from ref. 120 Copyright 2018 Elsevier.

Thickness of perovskite [nm]	V _{OC} ^b [V]	J _{SC} ^b [mA cm ⁻²]	FF ^b	PCE ^b [%]	Integrated J _{SC} [mA cm ⁻²]
400	0.62 ± 0.02 (0.63)	7.88 ± 0.27 (8.15)	0.33 ± 0.03 (0.35)	1.72 ± 0.186 (1.75)	8.03
600	0.82 ± 0.02 (0.84)	12.18 ± 0.55 (12.69)	0.47 ± 0.02 (0.5)	4.86 ± 0.01 (5.17)	11.34
600 ^a	0.88 ± 0.01 (0.89)	12.44 ± 0.38 (12.91)	0.49 ± 0.03 (0.51)	5.55 (5.72)	12.28

^a Solvent annealed devices.

^b Values in parenthesis are the best results.

is not an easy process, and special care should be taken to avoid damage on the device during the weaving process. Finally, in wearable applications typically only one side of the weaved FSSC will be illuminated by sunlight; while the back side will be dark. Therefore, the applications of these fiber-shaped solar cells are more preferred to the wearable applications due to their three dimensions' absorption property. As an alternative, the PV materials could be developed on the textile substrates, instead of weaving FSSC into textiles as the textile-based PSSCs, which is an innovative area that overcomes some of the challenges of FSSC technology. However, one of the challenges is the integration of a stable and uniform planar layer, which also leads to the relatively planar electrodes required for device fabrication. Evidently, device processes that can be conducted at low temperatures are necessary in the final development of the textile solar cells. The fabricated textile-based PSSCs solar cell should finally be super-flexible, light-weight, wearable, formable and foldable, which potentially hampers the barrier encapsulation requirements. Here, the routes that address highly stable active layer materials should be still considered, at least before the textile solar cells can reach a production stage. As application areas, the PSSCs textile-based solar cells are recommended as the power harvesting part of smart textiles, e-textiles, and wearable electronic devices, due to their compatibility with wearable electronic applications. The PSSCs textile-based solar cells could be used in emergency situations, such as for temporary tents used in floods, earthquakes, and other climate change related emergencies, where the requirements of light-weight and easy installation can be very beneficial. They could also be applied in everyday households as solar curtains for supplying the electrical energy required during the daytime. Although just a few prototypes of textile-based PSSCs solar cells have been fabricated so far, up-scaling of these devices still needs more efforts in order to reach an optimization of the fabrication process from the prospective of the materials and the employed fabrication techniques. The first challenge in developing textile solar cells as a power-harvesting unit in smart textiles and e-textiles is to develop nontoxic DSSCs, OPV, and PSCs. One way in this direction would be relying on natural dyes, nontoxic organic materials,

and lead-free perovskites in the future. On the other hand, eco-friendly approaches for fabricating textile solar cells might lead to less efficient devices. Retaining the super-flexibility of textile-based PSSCs solar cells upon devices encapsulation is another challenge, which should be thoroughly investigated by scientist. Here, standard R2R processing techniques are well suited, with a variety of available thin-film coating techniques available both for solution processing and vacuum evaporation methods. It should be noted that in the device configurations employed for textile-based PSSCs solar cells, ultrahigh mechanical flexibilities are sought for, which potentially hampers the requirements on device encapsulation. Typically, these organic and hybrid solar cells are encapsulated with rigid or only partially flexible barrier layers in order to prevent the material from photooxidation processes, i.e. when chemical degradation takes place upon contact with oxygen and light. As the devices are required to be more flexible, it automatically comes along with lower barrier properties, which is a potential challenge for the stability of these devices. One route to alleviate this trade-off could be the addition of additive assisted stabilizers added into the active layers of the devices [121,122]. This has been demonstrated as a very promising route for organic solar cells, highlighting that one can reach longer device stability with lower barrier requirements [123–125]. Finally, the efficiency remains as a key challenge for making textile-based PSSCs solar cells for real wearable applications, which should be maximized to supply the required electrical energy for the relevant electronic devices. To achieve this, many more research efforts should be devoted in the future.

Declaration of competing interest

The authors declare that they have no known competing financial interests or personal relationships that could have appeared to influence the work reported in this paper.

Table 13
Structure and PV parameters of different types of fabricated textile-based PSSCs.

Structure	Type	J _{SC} (mA cm ⁻²)	V _{OC} (V)	FF	PCE (%)	Ref.
FTO coated glass/ TiO ₂ NPs/N719/I ⁻ I ₃ /PPY/Ni-Coated fabric	DSSC	9.60	0.652	0.52	3.30	[107]
FTO coated glass/ P25+TNT/TiO ₂ blocking layer/ TiO ₂ NPs/gel electrolyte/E- MWCNTs coated fabric	DSSC	11.92	0.688	0.69	5.69	[108]
FTO coated glass/ TNT + TiO ₂ NPs/ gel electrolyte/ HC-GCF/PET	DSSC	14.75	0.660	0.71	6.93	[109]
FTO coated glass/ TNT + TiO ₂ NPs/ gel electrolyte/AC doped MWNT fabric coated	DSSC	12.03	0.766	0.79	7.29	[110]
FTO coated glass/ TiO ₂ NPs/gel electrolyte/M-AC- MCNT fabric coated	DSSC	12.4	0.72	0.70	6.26	[111]
TiO ₂ DLP metal ribbon coated/ electrolyte/Pt- NPLCY	DSSC	5.78	0.725	0.63	2.63	[112]
Pt-ITO coated PEN/ electrolyte/dye sensitized TiO ₂ / Ti/PA coated glass fabric	DSSC	5.10	0.790	0.27	1.10	[113]
Gold textile electrode/MoO ₃ / P ₃ T:PCBM/ZnO/ ITO coated flexible film	OPV	13.11	0.57	0.24	1.79	[114]
Al/P3HT:PCBM/ PEDOT:PSS coated fabric	OPV	8.50	0.560	0.46	2.20	[115]
AZO-Ag-AZO coated PET/P ₃ HT:PCBM/ PEDOT:PSS HTL/ PEDOT:PSS F ET/ Fabric of metal and polymer fibers	OPV	5.00	0.570	0.53	1.50	[116]
Ag NW/PEDOT:PSS/ P3HD:ICBA/ZnO- NP/Pressed Ag NW/IF fabric	OPV	0.26	0.410	0.25	0.02	[117]
Ag NW/PEDOT:PSS/ Active layer/ZnO- NP/Ag-NP/Fabric	OPV	3.44	0.500	0.24	0.40	[118]
ITO coated PEN/ SnO ₂ /PCBM/ MAPbI ₃ /Spiro- OmeTAD/Au/ Fabric	Perovskite	20.53	1.060	0.66	14.30	[119]
Ag/PCBM/MAPbI ₃ / PEDOT:PSS/ PEDOT:PSS-CNT/ PUR/Fabric	Perovskite	12.69	0.820	0.50	5.17	[120]

Acknowledgements

This work was funded by the National Natural Science Foundation of China (NSFC), No. 61774046. It was also supported by Talented Young Scientist Program (TYSF) in China. Mohammad Hatamvand would like to express his special thanks of gratitude to TYSF and Fudan University

for their intellectual and financial support. Morten Madsen acknowledges Danmarks Frie Forskningsfond, DFF FTP for funding of the project React-PV, No. 8022-00389B. Paola Vivo acknowledges the financial support of Business Finland, project “Solar WAVE” and Jane & Aatos Erkko Foundation, project “ASPIRE”. This work is part of the Academy of Finland Flagship Program, Photonics Research and Innovation (PREIN, Decision number 320165).

Mónica Lira-Cantú acknowledges the Spanish MINECO for the grant GraPErOs (ENE2016-79282-C5-2-R).

References

- A.A. Memon, et al., Carbonous metallic framework of multi-walled carbon Nanotubes/Bi2S3 nanorods as heterostructure composite films for efficient quasi-solid state DSSCs, *Electrochim. Acta* 283 (2018) 997–1005, <https://doi.org/10.1016/j.electacta.2018.04.131>.
- I.A. Sahito, et al., Graphene nanosheets as counter electrode with phenoxazine dye for efficient dye sensitized solar cell, *Org. Electron.* 44 (2017) 32–41, <https://doi.org/10.1016/j.orgel.2017.01.035>.
- Y. Ren, et al., A stable blue photosensitizer for color palette of dye-sensitized solar cells reaching 12.6% efficiency, *J. Am. Chem. Soc.* 140 (7) (2018) 2405–2408, <https://doi.org/10.1021/jacs.7b12348>.
- W. Lu, et al., Porous N-doped-carbon coated CoSe₂anchored on carbon cloth as 3D photocathode for dye-sensitized solar cell with efficiency and stability outperforming Pt, *Nano Res.* 12 (2019) 159–163, <https://doi.org/10.1007/s12274-018-2195-5>.
- H. Jing, et al., Onion-like graphitic carbon covering metallic nanocrystals derived from brown coal as a stable and efficient counter electrode for dye-sensitized solar cells, *J. Power Sources* 414 (2019) 495–501, <https://doi.org/10.1016/j.jpowsour.2019.01.042>.
- T.M.W.J. Bandara, et al., High efficiency dye-sensitized solar cell based on a novel gel polymer electrolyte containing Rbl and tetrahexylammonium iodide (Hex 4 NI) salts and multi-layered photoelectrodes of TiO₂ nanoparticles, *Renew. Sustain. Energy Rev.* 103 (2019) 282–290, <https://doi.org/10.1016/j.rser.2018.12.052>.
- Y. Huang, et al., Single-layer TiO₂Film composed of mesoporous spheres for high-efficiency and stable dye-sensitized solar cells, *ACS Sustain. Chem. Eng.* 6 (3) (2018) 3411–3418, <https://doi.org/10.1021/acssuschemeng.7b03626>.
- W. Zhang, et al., Comprehensive control of voltage loss enables 11.7% efficient solid-state dye-sensitized solar cells, *Energy Environ. Sci.* 11 (7) (2018) 1779–1787, <https://doi.org/10.1039/C8EE00661J>.
- P. Wang, et al., Stable and efficient organic dye-sensitized solar cell based on ionic liquid electrolyte, *Joule* 2 (10) (2018) 2145–2153, <https://doi.org/10.1016/j.joule.2018.07.023>.
- B. Xu, et al., Solution-processed nanoporous NiO-dye-ZnO photocathodes: toward efficient and stable solid-state p-type dye-sensitized solar cells and dye-sensitized photoelectrosynthesis cells, *Nano Energy* 55 (2019) 59–64, <https://doi.org/10.1016/j.nanoen.2018.10.054>.
- S. Rafique, et al., Fundamentals of bulk heterojunction organic solar cells: an overview of stability/degradation issues and strategies for improvement, *Renew. Sustain. Energy Rev.* 84 (2018) 43–53, <https://doi.org/10.1016/j.rser.2017.12.008>.
- A. Ali, et al., Laminated carbon nanotubes for the facile fabrication of cost-effective polymer solar cells, *ACS Appl. Energy Mater.* 1 (3) (2018) 1226–1232, <https://doi.org/10.1021/acsaelm.7b00345>.
- N. Gasparini, et al., The physics of small molecule acceptors for efficient and stable bulk heterojunction solar cells, *Adv. Energy Mater.* 8 (12) (2018), 1703298, <https://doi.org/10.1002/aenm.201703298>.
- M.B. Upama, et al., Effect of annealing dependent blend morphology and dielectric properties on the performance and stability of non-fullerene organic solar cells, *Sol. Energy Mater. Sol. Cell.* 176 (2018) 109–118, <https://doi.org/10.1016/j.solmat.2017.11.027>.
- M. Mirsafaei, et al., Sputter-deposited titanium oxide layers as efficient electron selective contacts in organic photovoltaic devices, *ACS Appl. Energy Mater.* 3 (1) (2020) 253–259, <https://doi.org/10.1021/acsaelm.9b01454>.
- E. Destouesse, et al., Slot-die processing and encapsulation of non-fullerene based ITO-free organic solar cells and modules, *Flex. Print. Electron.* 4 (2019), <https://doi.org/10.1088/2058-8585/ab556f>.
- S. Li, et al., An unfused-core-based nonfullerene acceptor enables high-efficiency organic solar cells with excellent morphological stability at high temperatures, *Adv. Mater.* 30 (6) (2018), <https://doi.org/10.1002/adma.201705208>.
- X. Du, et al., Efficient polymer solar cells based on non-fullerene acceptors with potential device lifetime approaching 10 years, *Joule* 3 (1) (2019) 215–226, <https://doi.org/10.1016/j.joule.2018.09.001>.
- B.R. Patil, et al., ITO with embedded silver grids as transparent conductive electrodes for large area organic solar cells, *Nanotechnology* 28 (40) (2017), 405303, <https://doi.org/10.1088/1361-6528/aa820a>.
- L. Ciammaruchi, et al., Stability of organic solar cells with PCDTBT donor polymers: an interlaboratory study, *J. Mater. Res.* 33 (2018) 1909–1924, <https://doi.org/10.1557/jmr.2018.163>.

- [21] M. Ahmadpour, et al., Crystalline molybdenum oxide layers as efficient and stable hole contacts in organic photovoltaic devices, *ACS Appl. Energy Mater.* 2 (1) (2019) 420–427, <https://doi.org/10.1021/acsae.8b01452>.
- [22] Q. An, et al., High-efficiency and air stable fullerene-free ternary organic solar cells, *Nano Energy* 45 (2018) 177–183, <https://doi.org/10.1016/j.nanoen.2017.12.050>.
- [23] L. Ye, et al., Surpassing 10% efficiency benchmark for nonfullerene organic solar cells by scalable coating in air from single nonhalogenated solvent, *Adv. Mater.* 30 (8) (2018), 1705485, <https://doi.org/10.1002/adma.201705485>.
- [24] H.K.H. Lee, et al., Stability study of thermal cycling on organic solar cells, *J. Mater. Res.* 33 (13) (2018) 1902–1908, <https://doi.org/10.1557/jmr.2018.167>.
- [25] D. Wang, et al., MoS₂ incorporated hybrid hole transport layer for high performance and stable perovskite solar cells, *Synth. Met.* 246 (2018) 195–203, <https://doi.org/10.1016/j.synthmet.2018.10.012>.
- [26] X. Li, et al., A stable lead halide perovskite nanocrystals protected by PMMA, *Sci. China Mater.* 61 (2018) 363–370, <https://doi.org/10.1007/s40843-017-9148-7>.
- [27] M. Shirazi, et al., Fabrication of hole-conductor-free perovskite solar cells based on Al doped ZnO and low-cost carbon electrode, *J. Mater. Sci. Mater. Electron.* 29 (2018) 10092–10101, <https://doi.org/10.1007/s10854-018-9054-8>.
- [28] T.T. Ngo, et al., Spray-pyrolyzed ZnO as electron selective contact for long term stable planar CH₃NH₃PbI₃ perovskite solar cells, *ACS Appl. Energy Mater.* 1 (8) (2018), <https://doi.org/10.1021/acsae.8b00733>.
- [29] A. Mei, et al., A hole-conductor-free, fully printable mesoscopic perovskite solar cell with high stability, *Science* 345 (6194) (2014) 295–298, <https://doi.org/10.1126/science.1254763>.
- [30] M. Konstantakou, et al., Anti-solvent crystallization strategies for highly efficient perovskite solar cells, *Crystals* 7 (2017) 291, <https://doi.org/10.3390/cryst7100291>.
- [31] P.S. Chandrasekhar, et al., Higher efficiency perovskite solar cells using 2 core-shell nanoparticles, *Sustain. Energy Fuels* 2 (10) (2018) 2260–2267, <https://doi.org/10.1039/C7SE00472A>.
- [32] J. Cheng, et al., Highly efficient planar perovskite solar cells achieved by simultaneous defect engineering and formation kinetic control, *J. Mater. Chem. A* 6 (46) (2018) 23865–23874, <https://doi.org/10.1039/C8TA08819E>.
- [33] Y. Hua, et al., Composite hole-transport materials based on a metal-organic copper complex and spiro-OMeTAD for efficient perovskite solar cells, *Solar RRL* 2 (2018), <https://doi.org/10.1002/solr.201700073>.
- [34] M.V. Khenkin, et al., Reconsidering figures of merit for performance and stability of perovskite photovoltaics, *Energy Environ. Sci.* 11 (4) (2018) 739–743, <https://doi.org/10.1039/C7EE02956J>.
- [35] K. Mahmood, et al., Electrosprayed polymer-hybridized multidoped ZnO mesoscopic nanocrystals yield highly efficient and stable perovskite solar cells, *ACS Omega* 3 (8) (2018) 9648–9657, <https://doi.org/10.1021/acsomega.8b01412>.
- [36] A. Mingorance, et al., Interfacial engineering of metal oxides for highly stable halide perovskite solar cells, *Adv. Mat. Int.* 5 (2018), <https://doi.org/10.1002/admi.201800367>.
- [37] M.A. Mahmud, et al., A high performance and low-cost hole transporting layer for efficient and stable perovskite solar cells, *Phys. Chem. Chem. Phys.* 19 (31) (2017) 21033–21045, <https://doi.org/10.1039/C7CP03551A>.
- [38] N. Aeineh, et al., Optical optimization of the TiO₂Mesoporous layer in perovskite solar cells by the addition of SiO₂Nanoparticles, *ACS Omega* 3 (8) (2018) 9798–9804, <https://doi.org/10.1021/acsomega.8b01119>.
- [39] N.J. Jeon, et al., Solvent engineering for high-performance inorganic-organic hybrid perovskite solar cells, *Nat. Mater.* 13 (2014) 897–903, <https://doi.org/10.1038/nmat4014>.
- [40] N. Islavath, G. Lingamallu, The performance enhancement of HTM-free ZnO nanowire-based perovskite solar cells via low-temperature TiCl₄treatment, *Sol. Energy* 170 (2018) 158–163, <https://doi.org/10.1016/j.solener.2018.05.050>.
- [41] A. Fakhruddin, et al., Perovskite-polymer blends influencing microstructure, non-radiative recombination pathways and photovoltaic performance of perovskite solar cells, *ACS Appl. Mater. Interfaces* 10 (49) (2018) 42542–42551, <https://doi.org/10.1021/acsami.8b18200>.
- [42] Y. Saygili, et al., Planar perovskite solar cells with high open-circuit voltage containing a supramolecular iron complex as hole transport material dopant, *ChemPhysChem* 19 (11) (2018) 1363–1370, <https://doi.org/10.1002/cphc.201800032>.
- [43] F. Zhang, et al., Dopant-free star-shaped hole-transport materials for efficient and stable perovskite solar cells, *Dyes Pigments* 136 (2017) 273–277, <https://doi.org/10.1016/j.dyepig.2016.08.002>.
- [44] J. Qin, et al., The optimum titanium precursor of fabricating TiO₂compact layer for perovskite solar cells, *Nanoscale Res. Lett.* 12 (1) (2017), <https://doi.org/10.1186/s11671-017-2418-9>.
- [45] L. Li, et al., Recent advances of flexible perovskite solar cells, *J. Energy Chem.* 27 (3) (April, 2018) 673–689, <https://doi.org/10.1016/j.jechem.2018.01.003>.
- [46] Z. Zhang, et al., All-carbon electrodes for flexible solar cells, *Appl. Sci.* 8 (2018) 152, <https://doi.org/10.3390/app8020152>.
- [47] J. Yoon, et al., Superflexible, high-efficiency perovskite solar cells utilizing graphene electrodes: towards future foldable power sources, *Energy Environ. Sci.* 10 (1) (2017) 337–345, <https://doi.org/10.1039/C6EE02650H>.
- [48] I.K. Popoola, et al., Recent progress in flexible perovskite solar cells: materials, mechanical tolerance and stability, *Renew. Sustain. Energy Rev.* 82 (2018) 3127–3151, <https://doi.org/10.1016/j.rser.2017.10.028>.
- [49] P.D. Lund, et al., Application of dye-sensitized and perovskite solar cells on flexible substrates, *Flex. Print. Electron.* 3 (2018), <https://doi.org/10.1088/2058-8585/aaabc9>. IOP Publishing.
- [50] J.Y. Lam, et al., A stable, efficient textile-based flexible perovskite solar cell with improved washable and deployable capabilities for wearable device applications, *RSC Adv.* 7 (86) (2017) 54361–54368, <https://doi.org/10.1039/C7RA10321B>.
- [51] T. Jayenta Singh, et al., Flexible organic solar cells with graphene/PEDOT:PSS Schottky junction on PET substrates, *Optik* 181 (2019) 984–992, <https://doi.org/10.1016/j.ijleo.2018.12.179>.
- [52] X. Zhang, et al., Extremely lightweight and ultra-flexible infrared light-converting quantum dot solar cells with high power-per-weight output using a solution-processed bending durable silver nanowire-based electrode, *Energy Environ. Sci.* 11 (2) (2018) 354–364, <https://doi.org/10.1039/C7EE02772A>.
- [53] F. Di Giacomo, et al., Progress, challenges and perspectives in flexible perovskite solar cells, *Energy Environ. Sci.* 9 (10) (2016) 3007–3035, <https://doi.org/10.1039/C6EE01137C>.
- [54] S. Guterman, et al., Optimized flexible cover films for improved conversion efficiency in thin film flexible solar cells, *Opt. Mater.* 79 (2018) 243–246, <https://doi.org/10.1016/j.optmat.2018.03.034>.
- [55] J.H. Heo, et al., Highly efficient low temperature solution processable planar type CH₃NH₃PbI₃perovskite flexible solar cells, *J. Mater. Chem.* 4 (5) (2016) 1572–1578, <https://doi.org/10.1039/C5TA09520D>.
- [56] J.H. Heo, et al., Highly flexible, high-performance perovskite solar cells with adhesion promoted AuCl₃-doped graphene electrodes, *J. Mater. Chem.* 5 (40) (2017) 21146–21152, <https://doi.org/10.1039/C7TA06465A>.
- [57] J.H. Heo, et al., Super-flexible bis(trifluoromethanesulfonyl)-amide doped graphene transparent conductive electrodes for photo-stable perovskite solar cells, *J. Mater. Chem.* 6 (18) (2018) 8251–8258, <https://doi.org/10.1039/C8TA02672F>.
- [58] Y. Hu, et al., Highly efficient flexible solar cells based on a room-temperature processed inorganic perovskite, *J. Mater. Chem.* 6 (41) (2018) 20365–20373, <https://doi.org/10.1039/C8TA06719H>.
- [59] C. Kamaraki, et al., Efficient flexible printed perovskite solar cells based on lead acetate precursor, *Sol. Energy* 176 (2018) 406–411, <https://doi.org/10.1016/j.solener.2018.10.055>.
- [60] M. Khadem, et al., Highly transparent micro-patterned protective coatings on polyethylene terephthalate for flexible solar cell applications, *Sol. Energy* 171 (2018) 629–637, <https://doi.org/10.1016/j.solener.2018.07.023>.
- [61] J.H. Kim, et al., Flexible ITO films with atomically flat surfaces for high performance flexible perovskite solar cells, *Nanoscale* 10 (44) (2018) 20587–20598, <https://doi.org/10.1039/C8NR06586A>.
- [62] G. Li, et al., Engineering flexible dye-sensitized solar cells for portable electronics, *Sol. Energy* 177 (2019) 80–98, <https://doi.org/10.1016/j.solener.2018.11.017>.
- [63] X. Fu, et al., Flexible solar cells based on carbon nanomaterials, *Carbon* 139 (2018) 1063–1073, <https://doi.org/10.1016/j.carbon.2018.08.017>.
- [64] Z. Wu, et al., Flexible and stretchable perovskite solar cells: device design and development methods, *Small Methods* 2 (7) (2018), <https://doi.org/10.1002/smtd.201800031>.
- [65] T. Lv, et al., Wearable fiber-shaped energy conversion and storage devices based on aligned carbon nanotubes, *Nano Today* 11 (5) (2016) 644–660, <https://doi.org/10.1016/j.nantod.2016.08.010>.
- [66] M. Stoppa, A. Chiolerio, Wearable electronics and smart textiles: a critical review, *Sensors* 14 (7) (2014) 11957–11992, <https://doi.org/10.3390/s140711957>.
- [67] I.A. Sahito, A. Khatri, *Smart and Electronic Textiles. Advanced Textile Testing Techniques*, CRC Press, 2017, pp. 295–314.
- [68] M. Peng, et al., Three dimensional photovoltaic fibers for wearable energy harvesting and conversion, *J. Energy Chem.* 27 (3) (2018) 611–621, <https://doi.org/10.1016/j.jechem.2018.01.008>.
- [69] T. Chen, et al., Novel solar cells in a wire format, *Chem. Soc. Rev.* 42 (12) (2013) 5031–5041, <https://doi.org/10.1039/C3CS35465B>.
- [70] M. Hösel, The solar textile challenge: how it will not work and where it might, *ChemSusChem* 8 (6) (2015) 966–969, <https://doi.org/10.1002/cssc.201403377>.
- [71] R. Mather, J. Wilson, Fabrication of photovoltaic textiles, *Coatings* 7 (5) (2017) 63, <https://doi.org/10.3390/coatings7050063>.
- [72] S.J. Varma, et al., Fiber-type solar cells, nanogenerators, batteries, and supercapacitors for wearable applications, *Adv. Sci.* 5 (9) (2018), <https://doi.org/10.1002/advs.201800340>.
- [73] D. Zou, et al., Fiber-shaped flexible solar cells, *Coord. Chem. Rev.* 254 (9–10) (2010) 1169–1178, <https://doi.org/10.1016/j.ccr.2010.02.012>.
- [74] X. Pu, et al., Wearable power-textiles by integrating fabric triboelectric nanogenerators and fiber-shaped dye-sensitized solar cells, *Adv. Energy Mater.* 6 (20) (2016), <https://doi.org/10.1002/aenm.201601048>.
- [75] G. Liu, et al., Hierarchically structured photoanode with enhanced charge collection and light harvesting abilities for fiber-shaped dye-sensitized solar cells, *Nano Energy* 49 (2018) 95–102, <https://doi.org/10.1016/j.nanoen.2018.04.037>.
- [76] H. Li, et al., Stable hydrophobic ionic liquid gel electrolyte for stretchable fiber-shaped dye-sensitized solar cell, *ChemNanoMat* 1 (6) (2015) 399–402, <https://doi.org/10.1002/cnma.201500093>.
- [77] L. Chen, et al., One-step growth of CoNi₂S₄ nanoribbons on carbon fibers as platinum-free counter electrodes for fiber-shaped dye-sensitized solar cells with high performance: polymorph-dependent conversion efficiency, *Nano Energy* 11 (2015) 697–703, <https://doi.org/10.1016/j.nanoen.2014.11.047>.
- [78] W. Song, et al., Improving the photovoltaic performance and flexibility of fiber-shaped dye-sensitized solar cells with atomic layer deposition, *Nano Energy* 19 (2016) 1–7, <https://doi.org/10.1016/j.nanoen.2015.11.006>.

- [79] Z. Wen, et al., Self-powered textile for Wearable electronics by hybridizing fiber-shaped nanogenerators, solar cells, and supercapacitors, *Sci. Adv.* 2 (10) (2016), <https://doi.org/10.1126/sciadv.1600097>.
- [80] G. Liu, et al., Study on a stretchable, fiber-shaped, and TiO₂nanowire array-based dye-sensitized solar cell with electrochemical impedance spectroscopy method, *Electrochim. Acta* 267 (2018) 34–40, <https://doi.org/10.1016/j.electacta.2018.02.075>.
- [81] Z. Li, et al., Electrophoretic deposition of graphene-TiO₂hierarchical spheres onto Ti thread for flexible fiber-shaped dye-sensitized solar cells, *Mater. Des.* 105 (2016) 352–358, <https://doi.org/10.1016/j.matdes.2016.05.060>.
- [82] M. Peng, et al., Efficient fiber shaped zinc bromide batteries and dye sensitized solar cells for flexible power sources, *J. Mater. Chem. C* 3 (10) (2015) 2157–2165, <https://doi.org/10.1039/C4TC02997F>.
- [83] X. Fu, et al., A fiber-shaped solar cell showing a record power conversion efficiency of 10%, *J. Mater. Chem. 6* (1) (2017) 45–51, <https://doi.org/10.1039/C7TA08637G>.
- [84] T. Chen, et al., ‘An integrated ‘energy wire’ for both photoelectric conversion and energy storage, *Angew. Chem. Int. Ed.* 51 (48) (2012) 11977–11980, <https://doi.org/10.1002/anie.201207023>.
- [85] M. Peng, et al., Organic dye-sensitized photovoltaic fibers, *Sol. Energy* 150 (2017) 161–165, <https://doi.org/10.1016/j.solener.2017.04.007>.
- [86] M. Toivola, et al., Photovoltaic fiber, *Thin Solid Films* 517 (8) (2009) 2799–2802, <https://doi.org/10.1016/j.tsf.2008.11.057>.
- [87] M. Peng, D. Zou, Flexible fiber/wire-shaped solar cells in progress: properties, materials, and designs, *J. Mater. Chem.: Mater. Energy Sustain.* 3 (41) (2015) 20435–20458, <https://doi.org/10.1039/C5TA03731J>.
- [88] Z. Yang, et al., Stretchable, wearable dye-sensitized solar cells, *Adv. Mater.* 26 (17) (2014) 2643–2647, <https://doi.org/10.1002/adma.201400152>.
- [89] Z. Zhang, et al., Stretchable polymer solar cell fibers, *Small* 11 (6) (2015) 675–680, <https://doi.org/10.1002/smll.201400874>.
- [90] S. Greulich-Weber, et al., Textile solar cells based on SiC microwires, *Mater. Sci. Forum* (2009) 239–242, <https://doi.org/10.4028/www.scientific.net/MSF.61-5-617.239>.
- [91] M. Ebner, et al., Regenerated cellulose fiber solar cell, *Flex. Print. Electron.* 2 (1) (2017), <https://doi.org/10.1088/2058-8585/aa5707>.
- [92] Z. Zhang, et al., Weaving efficient polymer solar cell wires into flexible power textiles, *Adv. Energy Mater.* 4 (11) (2014), <https://doi.org/10.1002/aenm.201301750>.
- [93] L. Qiu, et al., Integrating perovskite solar cells into a flexible fiber, *Angew. Chem. Int. Ed.* 53 (39) (2014) 10425–10428, <https://doi.org/10.1002/anie.201404973>.
- [94] M. Lee, et al., Efficient fiber-shaped perovskite photovoltaics using silver nanowires as top electrode, *J. Mater. Chem. 3* (38) (2015) 19310–19313, <https://doi.org/10.1039/C5TA02779A>.
- [95] R. Li, et al., Wearable double-twisted fibrous perovskite solar cell, *Adv. Mater.* 27 (25) (2015) 3831–3835, <https://doi.org/10.1002/adma.201501333>.
- [96] S. He, et al., Radically grown obelisk-like ZnO arrays for perovskite solar cell fibers and fabrics through a mild solution process, *J. Mater. Chem. 3* (18) (2015) 9406–9410, <https://doi.org/10.1039/C5TA01532D>.
- [97] H. Hu, et al., Fiber-shaped perovskite solar cells with 5.3% efficiency, *J. Mater. Chem. 4* (10) (2016) 3901–3906, <https://doi.org/10.1039/C5TA09280A>.
- [98] L. Qiu, et al., Fiber-shaped perovskite solar cells with high power conversion efficiency, *Small* 12 (18) (2016) 2419–2424, <https://doi.org/10.1002/smll.201600326>.
- [99] L. Qiu, et al., An all-solid-state fiber-type solar cell achieving 9.49% efficiency, *J. Mater. Chem. 4* (26) (2016) 10105–10109, <https://doi.org/10.1039/C6TA03263J>.
- [100] X. Wang, et al., Wire-shaped perovskite solar cell based on TiO₂nanotubes, *Nanotechnology* 27 (20) (2016), <https://doi.org/10.1088/0957-4484/27/20/20LT01>.
- [101] H. Hu, et al., High performance fiber-shaped perovskite solar cells based on lead acetate precursor, *Sustain. Energy Fuels* 2 (1) (2017) 79–84, <https://doi.org/10.1039/C7SE00462A>.
- [102] H. Sun, et al., Novel graphene/carbon nanotube composite fibers for efficient wire-shaped miniature energy devices, *Adv. Mater.* 26 (18) (2014) 2868–2873, <https://doi.org/10.1002/adma.201305188>.
- [103] J. Deng, et al., Elastic perovskite solar cells, *J. Mater. Chem. 3* (42) (2015) 21070–21076, <https://doi.org/10.1039/C5TA06156C>.
- [104] S. Zhang, et al., Application of carbon fibers to flexible, miniaturized wire/fiber-shaped energy conversion and storage devices, *J. Mater. Chem. 5* (6) (2016) 2444–2459, <https://doi.org/10.1039/C6TA07868K>.
- [105] A. Balilonda, et al., Perovskite solar fibers: current status, issues and challenges, *Adv. Fiber Mater.* 1 (2) (2019) 101–125, <https://doi.org/10.1007/s42765-019-00011-0>.
- [106] Q. Shi, et al., Advanced functional fiber and smart textile, *Adv. Fiber Mater.* 1 (1) (2019) 3–31, <https://doi.org/10.1007/s42765-019-0002-z>.
- [107] J. Xu, et al., A flexible polypyrrole-coated fabric counter electrode for dye-sensitized solar cells, *J. Power Sources* 257 (2014) 230–236, <https://doi.org/10.1016/j.jpowsour.2014.01.123>.
- [108] A.A. Arbab, et al., Multiwalled carbon nanotube coated polyester fabric as textile based flexible counter electrode for dye sensitized solar cell, *Phys. Chem. Chem. Phys.* 17 (19) (2015) 12957–12969, <https://doi.org/10.1039/C5CP00818B>.
- [109] I.A. Sahito, et al., Flexible and conductive cotton fabric counter electrode coated with graphene nanosheets for high efficiency dye sensitized solar cell, *J. Power Sources* 319 (2016) 90–98, <https://doi.org/10.1016/j.jpowsour.2016.04.025>.
- [110] A.A. Arbab, et al., Fabrication of textile fabric counter electrodes using activated charcoal doped multi walled carbon nanotube hybrids for dye sensitized solar cells, *J. Mater. Chem. 4* (4) (2016) 1495–1505, <https://doi.org/10.1039/C5TA08858E>.
- [111] A.A. Memon, et al., Synthesis of highly photo-catalytic and electro-catalytic active textile structured carbon electrode and its application in DSSCs, *Sol. Energy* 150 (2017) 521–531, <https://doi.org/10.1016/j.solener.2017.04.052>.
- [112] M.J. Yun, et al., Insertion of dye-sensitized solar cells in textiles using a conventional weaving process, *Sci. Rep.* 18 (5) (2015), <https://doi.org/10.1038/srep11022>.
- [113] K. Opwis, et al., Preparation of a textile-based dye-sensitized solar cell, *Int. J. Photoenergy* (2016), <https://doi.org/10.1155/2016/3796074>.
- [114] S. Lee, et al., Stitchable organic photovoltaic cells with textile electrodes, *Nano Energy* 9 (2014) 88–93, <https://doi.org/10.1016/j.nanoen.2014.06.017>.
- [115] W. Kylberg, et al., Woven electrodes for flexible organic photovoltaic cells, *Adv. Mater.* 23 (8) (2011) 1015–1019, <https://doi.org/10.1002/adma.201003391>.
- [116] R. Stein, et al., Laminated fabric as top electrode for organic photovoltaics, *Appl. Phys. Lett.* 106 (2015), <https://doi.org/10.1063/1.4919940>.
- [117] S. Arumugam, et al., Fully spray-coated organic solar cells on woven polyester cotton fabrics for wearable energy harvesting applications, *J. Mater. Chem. A* 4 (2016) 5561–5568, <https://doi.org/10.1039/C5TA03389F>.
- [118] Y. Li, et al., Encapsulated textile organic solar cells fabricated by spray coating, *ChemistrySelect* 4 (1) (2019) 407–412, <https://doi.org/10.1002/slct.201803929>.
- [119] J.-Y. Lam, et al., A stable, efficient textile-based flexible perovskite solar cell with improved washable and deployable capabilities for wearable device applications, *RSC Adv.* 7 (86) (2017) 54361–54368, <https://doi.org/10.1039/C7RA10321B>.
- [120] J.W. Jung, et al., Fully solution-processed indium tin oxide-free textile-based flexible solar cells made of an organic–inorganic perovskite absorber: toward a wearable power source, *J. Power Sources* 402 (2018) 327–332, <https://doi.org/10.1016/j.jpowsour.2018.09.038>.
- [121] M. Bregnhøj, et al., Oxygen-dependent photophysics and photochemistry of prototypical compounds for organic photovoltaics: inhibiting degradation initiated by singlet oxygen at a molecular level, *Methods Appl. Fluoresc.* 8 (1) (2020), <https://doi.org/10.1088/2050-6120/ab4edc>.
- [122] V. Turkovic, et al., Biomimetic approach to inhibition of photooxidation in organic solar cells using beta-carotene as an additive, *ACS Appl. Mater. Interfaces* 11 (44) (2019) 41570–41579, <https://doi.org/10.1021/acsami.9b13085>.
- [123] V. Turkovic, et al., Long-term stabilization of organic solar cells using hindered phenols as additives, *ACS Appl. Mater. Interfaces* 6 (21) (2014) 18525–18537, <https://doi.org/10.1021/am5024989>.
- [124] V. Turkovic, et al., Long-term stabilization of organic solar cells using UV absorbers, *J. Phys. Appl. Phys.* 49 (2016), <https://doi.org/10.1088/0022-3727/49/12/125604>.
- [125] M. Salvador, et al., Suppressing photooxidation of conjugated polymers and their blends with fullerenes through nickel chelates, *Energy Environ. Sci.* 10 (9) (2017) 2005–2016, <https://doi.org/10.1039/C7EE01403A>.



Mohammad Hatamvand received his PhD degree in Textile Engineering from Yazd University, Iran in 2017. His PhD thesis was in the field of flexible solar cells and photovoltaic fibers. He was a visiting scholar at the University of Borås, Sweden from 2016 to 2017. He also did research as an external researcher at Bielefeld University of Applied Sciences, Germany from 2017 to 2019. He is currently a postdoctoral research fellow at Fudan University in Shanghai, China. His research interest focuses on perovskite flexible and textile solar cells as a power harvesting in wearable electronic devices.



Ehsan Kamrani has received a BSc-degree in bioelectric, MSc-degree in electrical-control engineering, and his PhD-degree in biomedical engineering. His research focuses on realization of smart wearable/implantable/zero-effort biomedical systems/sensors using AI-enabled on-chip-integrated microelectronics and bio-optoelectronics. He was a post-doctoral research-fellow with Harvard-MIT and the Wellman-center-for-Photomedicine, Harvard medical school, and biomedical-Nanomaterials-laboratory at POSTECH. He has been working at Harvard, MIT, UofWaterloo, and SBU as assistant/adjunct professor, instructor, and team-lead, and served as CTO/CEO/VP in several medtech companies, where he is leading several active projects for developing innovative technologies by integration of microelectronics, bio-optics/photonics and biological system aiming at creating novel diagnostic/therapeutic instruments



Dr. Shahid Mehmood is currently pursuing his post-doctoral fellowship in Micro-Nano System Center School of Information Science & Technology (SIST) Fudan University, Shanghai, China. He has completed his first Post-Doctoral fellowship from Higher Institution Centre of Excellence, UM Power Energy Dedicated Advanced Centre, Wisma R&D University of Malaya, Kuala Lumpur, Malaysia. He has master degree leading to Ph.D. in Physics (material Science) from University of Malaya. He earned his first master's degree in electronics (Applied physics) from Sarhad University of Science and information technology, Peshawar, Pakistan and bachelor's degree in physics and mathematics from Government postgraduate college, Haripur, KPK, Pakistan.



Prof. Monica Lira-Cantu received her PhD in Chemistry (Materials Science) in 1997, from 1999-2001 she worked as permanent research scientist at ExxonMobil Research & Engineering (U.S.A.). Her work in the area of Photovoltaics stability/degradation initiated in 2004 during a scientific stay with Prof. Frederik Krebs at DTU in Denmark, where she worked on the long-term stability of polymer/oxide solar cells. She has been visiting scientist with Prof. Truls Norby at UNorway (2003) and with Prof. Shozo Yanagida at CAST in Japan (2006). She is currently Group Leader of the Nanostructured Materials for Photovoltaic Energy Group at the Catalan Institute of Nanoscience and Nanotechnology (ICN2) in Barcelona (Spain).



Dr. Numan Arshid received his PhD from the Physics department at the University of Malaya, Malaysia in 2018. He is currently Postdoctoral fellow at the Micro-Nano System, SIST, Fudan University, Shanghai and visiting Research fellow at Graphene & Advanced 2D Materials Research Group, Sunway University, Malaysia. His research is focused on the development of 2D materials and their exploitation for Electrochemical applications, especially electrochemical energy storage (Supercapacitors), conversion (solar cells), and electrochemical sensing applications.



Morten Madsen, Professor wsr at the University of Southern Denmark (SDU), SDU NanoSYD. Conducted a postdoc fellowship at Prof. Ali Javey lab, UC Berkeley, and started in 2011 the organic photovoltaics (OPV) group at SDU. Is also heading the SDU Roll-to-Roll facility that focuses on complete up-scaling of OPV. Holds around 60 peer-reviewed publications on these topics, including publications in Nature, Nature Energy, Energy & Environ. Sci., Advanced Materials, etc. Coordinator and PI of the EU ITN Marie Curie network THINFACE, and currently PI on the EU Interreg project RollFlex, and on several national research projects (DFF FTP and Villum).



Irfan Ahmed received his PhD in Advanced Materials from University Malaysia Pahang, Malaysia in 2017. He is lecturer in Physics at Higher Education Department, KPK, Pakistan. Currently, he is postdoctoral research fellow in Prof. Yiqiang Zhan Group at Center of Micro-Nano System, School of Information Science and Technology (SIST) Fudan University, Shanghai. His research interests include synthesis of various morphological nanostructures through solution based and electrospinning techniques; fabrication of dye sensitized and perovskite solar cells; flexible solar devices and ultrafast time resolved spectroscopy of excited states and charge carrier dynamics in perovskite solar cell materials.



Bhushan Ramesh Patil received his Ph.D. in Engineering Science from the University of Southern Denmark in 2017. He received his BE in Electronics and Telecommunications in 2010 from the University of Mumbai, India and M.Sc. degree in Micro and Nano Systems from Technische Universitaet Chemnitz, Germany in 2014. He is working as a postdoctoral researcher at the University of Southern Denmark and his research interests include: Sheet-to-sheet/Roll-to-roll fabrication of Organic solar cells as well as interfacial layers and semi-transparent electrodes for large area flexible Organic Solar Cells.



Prof Dr Yiqiang Zhan (M) is a full professor of microelectronics at School of Information Science and Technology, Fudan University, Shanghai, China. He obtained his Ph.D. in physics from Fudan University, China in 2005 before moving to ISMN-CNR bologna, Italy as a postdoc. From 2007, he continued his research in Linkoping University, Sweden initially as a postdoc and then as an assistant professor. He joined Fudan University at 2011. He has a strong background in semiconductor physics and devices. His research team has expertise in novel semiconductor based solar cells, optoelectronics, sensors and memristive devices.



Paola Vivo is a Senior Research fellow at Tampere University (TAU), Finland. After pursuing her Ph.D. in Chemistry, she received Academy of Finland fellowship for postdoctoral research in 2013–2017. She currently leads the Hybrid Solar Cells research team at the Faculty of Engineering and Natural Sciences at TAU. Her research interests include developing novel organic materials and hybrid organic-inorganic systems for third generation solar cells, with current emphasis on halide perovskite photovoltaics.